We appreciate the thoughtful comments by referee #1. For discussion purposes we would like to respond to the general and detailed points raised.

Manuscript by Tauber et al. reports characterization of a new bipolar non-thermal plasma type charger for charging sub-15 nm aerosol particles. The main results of the study are measured size dependent charging efficiencies that are strongly biased to negative polarity, and mass and mobility characterization of the charger ions. Experimental data on sub-10 nm charging efficiencies are in the general interest in aerosol measurement techniques, while the current manuscript requires elaboration on several places prior to consideration for publication. General and specific comments are listed below

General:

- Experimental section: there is absolutely no description of the new plasma charger which is being characterized. This undermines the reproducibility of the most important results of the whole manuscript. The operation principle and general characteristics of the charger have to be described prior to publication. Otherwise a serious scientist in another lab cannot reproduce the potentially interesting results obtained with the charger. This applies also to the other used chargers.

There is indeed not much information given about the charger itself and we acknowledge that this is unusual for a research paper. However, we have to point out that there is still a patent pending and, thus, we cannot reveal all the technical details of how the charger works. Broadly speaking the atmospheric pressure plasma charger consists of a gas flow that is shielded by another gas flow from the surrounding atmosphere. The plasma is ignited inside the inner flow while the aerosol is administered through the outer gas stream. The main source of the plasma is a high-frequency copper electrode that is situated on the central axis of those two gas streams.

We will add the following description to the experimental section:
"The atmospheric pressure plasma charger consists of a gas flow that is shielded by another gas flow from the surrounding atmosphere. The plasma is ignited inside the inner flow while the aerosol is administered through the outer gas stream. The main source of the plasma is a high-frequency copper electrode that is situated on the central axis of those two gas streams.
According to Kallinger et al. (2012), the used radioactive 241Am charger has a cylindrical geometry with an axial flow direction. The radioactive source is mounted on the inner wall. The chamber has an inner diameter of about 30 mm and a length of 120 mm. Furthermore, the soft x-ray charger is composed of a stainless-steel tube and a photo ionizer. The aerosol particles are directed along the tube towards the soft x-ray source and leave the charger via an outlet, that is oriented perpendicularly to the axis of the tube. The tube has an inner diameter of 30 mm and a length of 200 mm."

- P8 L136 onward and P15 L223 onward, the authors discuss the effect of ion mass on the charging probability. They have even measured the ion masses and mobilities, while still in the theoretical prediction they use presumably "wrong" ion masses and mobilities. Why? Why not predicting the charging efficiencies with the measured ion mobility and mass? This is also speculated in the conclusions with statements that the charging efficiencies biased to negative polarity are explainable with the ion mobilities, while not a single ion mobility value (which should be actually weighed with the ion concentration) is reported even if they are measured.

We would like to thank the reviewer for making us aware of that and add the following to results section:
"In Table 1R the measured and calculated mean ion charger mobilities, mobility equivalent diameters, masses and ion mobility ratios are listed. For comparison the values found by Reischl et al. (1996) are also listed. The results were used to calculate the charge distribution with Fuchs theory as shown

in Figure 1R. Negatively charged particles in the size range from 4-12 nm by 241Am or X-Ray neutralizers agree well with the parameters derived by Reischl et al. (1996) and an ion mobility ratio of 1. For positively charged particles the charging efficiency is below the measurement results for particles between 4-10 nm. By correcting the charge distribution with the parameters derived by Reischl et al. (1996) with an ion mobility ratio of 0.8 the negatively charged particles with a size below 4 nm fit perfectly to theory. The measurement results of this work reveal an increased charging efficiency for both polarities as shown in Figure 1R. For mobility equivalent diameters between 4 and 12 nm and positive polarity the charging efficiency fits with theory for 241Am, X-Ray and the plasma torch with air as working gas. In contrast to negatively charged particles where the results of the plasma torch with nitrogen or air as working gas above 7 nm is higher and below 7 nm is lower than expected by theory. Also, for 241Am, X-Ray and the plasma charger with helium the theory exceeds the measured charging efficiency. By correcting the theory with the acquired ion mobility ratio, a good agreement between theory and measurement can be found for negatively charged particles above 7 nm and for positively charged particles for the plasma torch with nitrogen as working gas. Although the effect for diameters > 7 nm can be explained, there is still a deviation for the smaller diameters from theory. The reported discrepancy can therefore not solely be attributed to the ion mobilities. There are other effects which should by investigated in further studies. Especially the charging effects below 5 nm which cause deviations from the charging model."

Table 1R. Comparison of ion cluster properties: polarity, mobility diameter Dp calculated from mean ion mobility Z, mean ion mass M and ion mobility ratio Z^-/Z^+.

	Polarity	Dp [nm]	Z [cm2/Vs]	M [Da]	Z^-/Z^+	
Reischl et al. (1996)	+	1.32	1.15	290	1.0	0.80
Reischl et al. (1996)	-	1.19	1.43	140	1.0	0.80
measured	+	1.07	1.76	356	1.0	0.66
measured	-	0.87	2.66	116	1.0	0.66

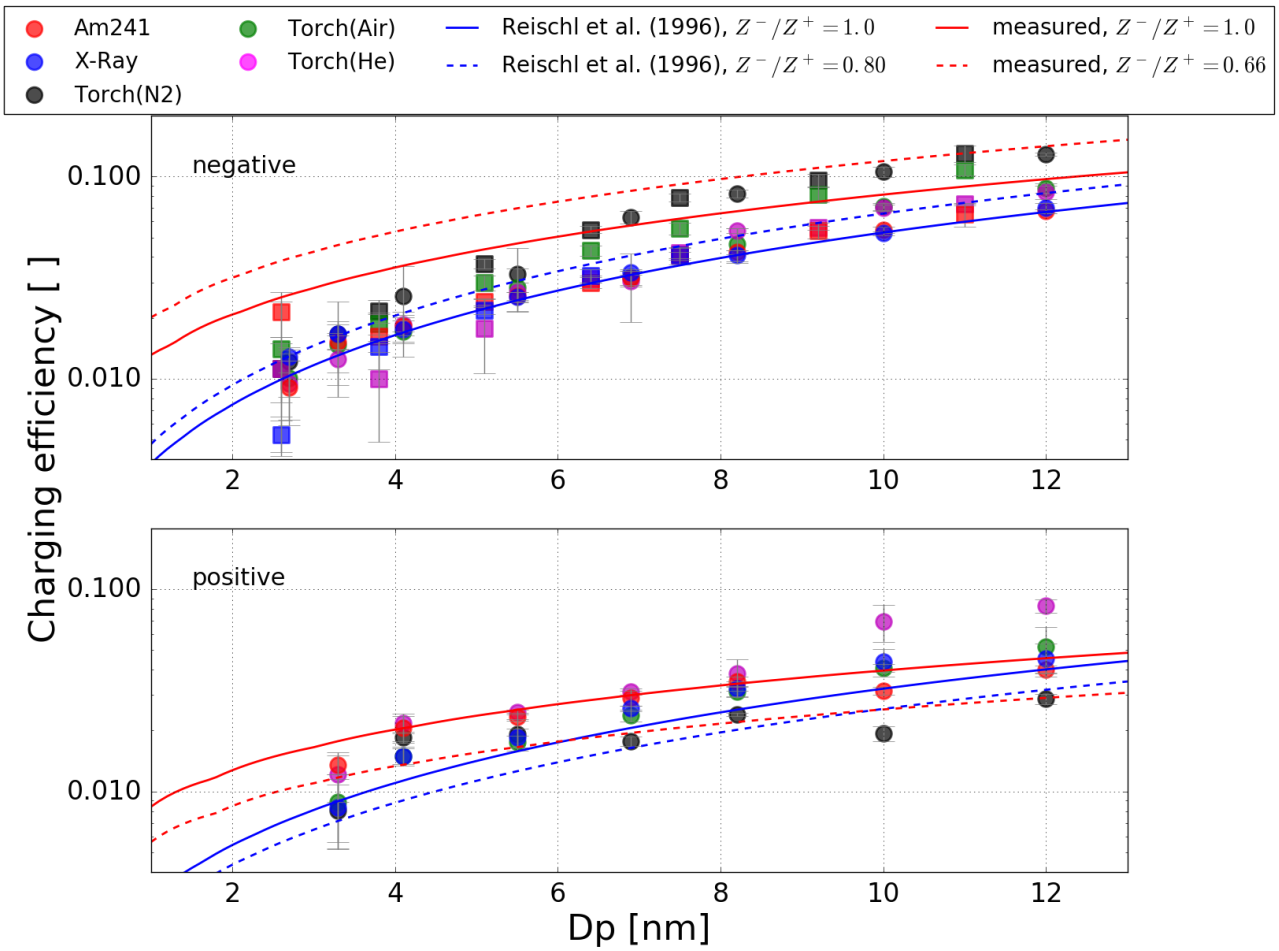

Figure 1R. Measured charging efficiencies for the different aerosol chargers for negatively and positively charged Ag particles (dots) and negatively charged NaCl particles (squares) with mobility diameters less than 12 nm. The lines represent the charge distribution according to Fuchs theory, the parameters for the ion mobilities, ion masses and ion mobility ratio are listed in table 1. The collision probability of ions was calculated following Hoppel and Frick (1986).

- Generally there are several experimental details that are not reported in sufficient detail, or statements of which interpretation is ambiguous. Some of these are picked below.

Specific:

- P1 L5, "increased charging efficiency", compared to what?

The sentence will be corrected:
"A comparison of the different neutralization methods revealed an increased charging efficiency for negatively charged particles using the non-radioactive plasma charger with nitrogen as working gas compared to a radioactive americium neutralizer."

- P1 L7, "charging mechanism", are you referring to the different neutralizers? Charging mechanism is a different thing

Yes, we refer to the different neutralizers.
The sentence will be corrected:
"The mobility and mass spectrometric measurements show that the generated neutralizer ions are of the same mobilities and composition independent of the examined neutralizer."

- P1 L8, in which sense the TSI X-ray is "standard" neutralizer? I would say commercial

The sentence will be corrected:
"It was the first time that the Gilbert Mark I plasma charger was characterized in comparison to a commercial TSI X-Ray (TSI Inc, Model 3088) and a radioactive americium neutralizer."

- P1 L9, "enhance" compared to what?

The sentence will be corrected:
"We observed that the plasma charger with nitrogen as working gas can enhance the charging probability for sub-10 nm particles compared to a radioactive americium neutralizer."

- P1 L10, "increased down towards", reformulate

The sentence will be corrected:
"Consequently, the limit of detection of differential or scanning mobility particle sizers can be increased to nanometer sized particles with the Gilbert Mark I plasma charger."

- P1 L20, "below 10 nm in diameter are typically difficult to neutralize", I would say the opposite

The sentence will be corrected:
"Aerosol particles below 10 nm in diameter are typically difficult to charge and carry only one electrical charge at maximum (Wiedensohler, 1988)."

- P1 L21, "Quantitative particle detection in this size range is extremely challenging due to high diffusional losses. Hence, a higher charging efficiency is of importance to improve the signal intensity in the sub-10 nm regime", the first sentence implies challenges in determining the diffusion losses, i.e. systematic uncertainty, while the second one deals with detection limit and poisson type random uncertainty. Improvements in the second does not help the first one.

We thank the reviewer for making us aware of this unclear formulation and the sentences will be reformulated:
"Quantitative particle detection in this size range is extremely challenging due to high diffusional losses, which results in low number concentrations. Therefore, a higher charging efficiency is of importance to increase the detectable number concentration in the sub-10 nm regime."

- P2 L33, it will be good to define what is non-thermal plasma, if it is the operation principle of the new charger

We fully agree with the referee on this point and added the following sentences to the manuscript:
"The term non-thermal plasma is usually used to describe a discharge in which the electrons are in thermal non-equilibrium with the ions. This means that the average temperature of the gas in such a discharge is far lower than the temperature of a thermal plasma (i.e. some hundred K compared to several thousand K in the latter case)."

- P2 L39, "mobility spectrum of . . .", it is the mobility spectrum of the charger ions, not of the chargers.

The sentence will be corrected:

"In the past, various studies have characterized the charging probabilities and mobility spectra of the charger ions produced by AC-corona, X-Ray or alpha-radiation based chargers (Wiedensohler et al., 1986; Steiner and Reischl, 2012; Kallinger et al., 2012; Kallinger and Szymanski, 2015)."

- P2 L46, "steady-state", earlier you talked about equilibrium, which one it is?

We measured the charging probability and assumed that the charge equilibrium inside the charger leads to a well-known size-dependent charge distribution. The chargers were measured during steady-state operational conditions. We will reformulate the sentence:
"Here we report on size-dependent charging probability measurements of a non-thermal plasma source (Gilbert Mark I plasma charger, Gruenwald Laboratories GmbH, Austria), an americium 241 (241Am) charger and of a TSI Advanced Aerosol Neutralizer 3088 by means of a tandem DMA (Differential Mobility Analyzer) setup as depicted in Figure 1."

- Figure 1, what is the sheath the flow rate and size resolution of the nDMAs? What about the furnace output distribution? How much the size resolution of the first DMA affects the results? Based on the plot, the DMA2 was operated with aerosol flow of 8 lpm at some point, can it really handle such high flow? Is it so that only the Torch requires the working gas? It is not clear from the figure. If the torch mixes helium with the sample flow, it changes the gas composition. Does it affect sizing of the DMA or the flow rates of the CPC? If yes, how was this accounted for?

The ratios for sheath flow and aerosol flow for the nDMA are listed below:
sheath flow 19.5 lpm / aerosol flow 2.5 lpm = 7.8
sheath flow 33.0 lpm / aerosol flow 5.0 lpm = 6.6
sheath flow 41 lpm / aerosol flow 8.0 lpm = 5.1

The furnace output distribution is constant because the 3 lpm through the furnace were not changed. The additional flow was introduced after the aerosol size classification and the aerosol distribution was checked before a measurement run to reach the desired concentration for the analyzed particle size. Both nDMAs are of identical construction and the classifier (nDMA 1) was always operating at the same sheath flow ratio (19.5 lpm / 3 lpm = 6.5). Consequently, we assume negligible effect of the size resolution of the first nDMA.

The geometric standard deviation of the particle size for the used nDMAs was evaluated by Winkler et al. (2008) for a sheath flow of 25 lpm and an aerosol flow of 4.6 lpm and is below 1.05 for particles with a mobility diameter down to 2 nm. The resulting flow ratio (25 / 4.6 = 5.4) is close to our measurement with 8 lpm aerosol flow and the signal-to-noise ratio was comparable to the measurements with lower aerosol flow rates.

Only the Torch requires an additional working gas, we will add the following sentence to the figure caption: "The additional working gas flow is only needed for the plasma charger."
The additional flow rate from the working gas is at max 1/9 of the aerosol flow. According to our measurements no sizing effects were observed. Since the generated charger ions are comparable, one can assume that the charged particles are comparable, and the sizing of the DMA is not affected. In addition, helium is an inert gas and therefore non-reactive and combine rapidly with the surrounding substances.

We will add the following paragraph in the experimental setup section:
"The geometric standard deviation of the particle size for the used nDMAs was evaluated by Winkler et al. (2008) for a sheath flow of 25 lpm and an aerosol flow of 4.6 lpm and is below 1.05 for particles with a mobility diameter down to 2 nm. The resulting flow ratio (sheath / aerosol = 5.4) is close to our measurement with 8 lpm aerosol flow and the signal-to-noise ratio was comparable to the

measurements with lower aerosol flow rates. The different flow settings for the nDMAs are listed in Table 2R."

Table 2R. Flow rates for the aerosol and sheath flow for the used nDMAs with the calculated sheath flow ratio.

nDMA	Aerosol flow [L/Min]	Sheath flow [L/Min]	Ratio
1	3.0	19.5	6.5
2	2.5	19.5	7.8
2	5.0	33.0	6.6
2	8.0	41.0	5.1

- P2 L56, which kind of ion trap?

The ion-trap used consists of two symmetrical half shells separated by an isolator. The charged ions and particles were removed by an ion-trap which was set to +/- 500 V. The capturing efficiency of the electrostatic precipitator was found to be > 99% in the size range between 1 and 10 nm (Brilke et al. 2020; Tauber et al., 2019b).

- P5 L93-94, "It can be concluded from the OES spectra that there is no ionization of aerosol particles facilitated by the carrier gas, since only neutral helium emission lines have been recorded." It is not clear what is the experimental setup during this experiment. It is only mentioned that helium is fed to the charger, there should be no particles in helium in the first place?

The optical emission spectrometer was located at the nozzle of the plasma charger and used to record spatially averaged optical data along the axis of the plasma source.

- P5 L94, "atoms from the copper high frequency antenna", what is this antenna?

We will add the following sentences on P5 L89 to explain the antenna and its usage:
"Thereby the plasma jet is shielded by another gas flow from the surrounding atmosphere. The plasma is ignited inside the inner flow while the aerosol is administered through the outer gas stream. The main source of the plasma is a high-frequency copper antenna/electrode that is situated on the central axis of those two gas streams."

- Section 2.1.1, what is the purpose of this section, or what we should conclude in terms of aerosol charging? Are the emission spectra comparable to the conditions of the charging efficiency experiments, or to the recorded mass spectra?

The emission spectra yield additional information about the charging mechanism and the plasma itself. The former encompasses the discovery that the charging of the aerosol particles is achieved via electrons that origin from the central electrode of the charger. The latter point includes, for example, the detection of singly charged He particles, which have a lifetime that is so short that they recombine before reaching the detector in the ioniAPi-TOF. On the other hand, the optical emission spectroscopy (OES) measurements were done in order to compare this novel charging mechanism to established ones like the X-ray or Americium chargers. Furthermore, the OES measurements led to a better understanding of the plasma behavior and, thus, the way of charge transfer from the plasma to the molecules or aerosols. The electrons are detached from the high-frequency copper electrode as those atoms are easily ionized. After leaving the electrode the charges attach themselves onto the preexisting molecules or aerosol particles. As a result, based on the ioniAPi-TOF and mobility measurements it can be shown that the different charging mechanism lead to comparable measurement results.

- P6 L103, "reduced temperature settings", what were the settings?
- P6 L107 "In Tauber et al. (2019b) the particle counting efficiency of the CPCs used here was determined, and the results obtained were corrected for the CPC detection efficiency", it is not clear what are used settings, since in the reference there are three different settings for the CPC.

We will change the following sentence and include the used temperature settings:
"Two butanol-based CPCs (TSI 3776 UCPC) with reduced temperature settings (Condenser 1.1°C, Saturator 30.1°C, Optics 31.1°C) compared to factory settings to increase the particle counting efficiency were used (Barmpounis et al., 2018; Tauber et al., 2019a)."

- P6 L100-110, the description of the experiment should be in section 2 where the setup is described. How what about losses in the dilution, how they were corrected? The second DMA scans the voltage, what is the CPC2 signal that is compared to the CPC1?

We will move P6 L100-110 to the experimental description section and exchange Figure 1 with the Figure R2 because of a misleading plot. The number concentration measurements were done after the dilution and not before as shown in the previous plot. The number concentration measurements of CPC 2 were inverted to calculate the number size distribution from the mobility distribution according to Petters et al. (2018), which was then compared to the average particle concentration measured by CPC 1.

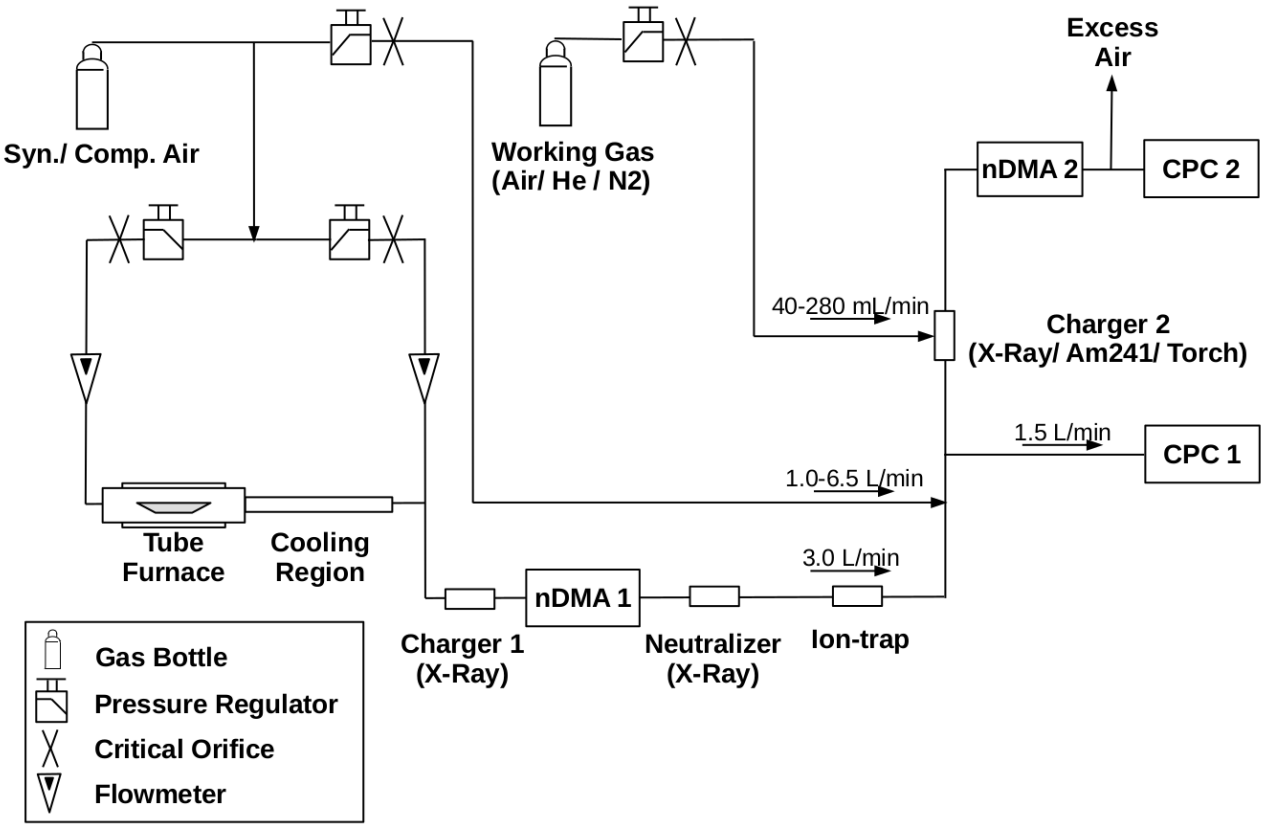

Figure 2R. Schematic of the experimental setup for the charging probability and particle size distribution inversion measurements. The additional working gas flow is only needed for the plasma charger.

- P6 L120, what the particle concentration has to do with charging efficiency? At extremely high concentrations concentration may affect the charging efficiency but not at low concentrations. Which CPC records the concentration that is mentioned? It is stated that data between 2-4 nm is

in agreement with theory. Then the next sentence states this is not true for NaCl particles. Which one is true? Please elaborate the whole paragraph

We will change the following paragraph accordingly:
"As the particle concentrations for very small diameters between 2-4nm are below 10000 #/ccm, the charging efficiencies of the different devices vary strongly at these particle sizes. The nDMA in this size range has a low transmission efficiency ranging from 20-55% and therefore the signal at the CPC 2 is very low. In addition, small temperature-fluctuations in the tube furnace lead to bigger uncertainties for the low total number concentration of the selected particle size. Especially for NaCl particles a big variation in the charging efficiencies of the different charging devices was observed. Those variations almost certainly are caused by the low number concentrations of NaCl particles at these sizes compared to Ag particles. However, except for NaCl particles at particle diameters between 2-4nm the associated data points for the 241Am neutralizer agree well with the approximations by Tigges et al. (2015) and Wiedensohler (1988)."

- P7 L129, agrees with what?

We will modify this sentence accordingly:
"Evidently, the data using helium agree well with theoretical approximations from Tigges et al. (2015) and Wiedensohler (1988) in the size regime between 4 and 10 nm."

- P7 L131, what is dependent on what?

We will modify this sentence accordingly:
"The data suggest no dependency of the charging efficiency on the charger ion polarity, when helium is used as working gas in the plasma torch."

- P8 L137 onward, also charger ion mobility should affect the charging probability.

Thank you for making us aware of this inconsistence, we change this sentence as follows:
"Wiedensohler and Fissan (1991) have shown that the predicted charging probabilities of NaCl and Ag particles strongly depend on the used carrier gas and the ion mass and mobility."

- P8 L143 "As Figure 3 shows, the plasma torch forms copper ions and free electrons which charge aerosol particles in the carrier gas." Why these are not observed in the mass spectrum?

The ions and free electrons are not observed in the mass spectrometer because their life time is far too short to reach the detector. For example, the transition probability of the ionization state represented by the copper emission line at 775.40 nm is 9×10^6 /s (Kramida et al., 2017). Thus, the mean lifetime of this ion is $1/(9 \times 10^6) \sim 0.1$ µs. Even if we assume a close to sonic flow velocity of the gas as an upper limit, the maximum range of the copper ion would be ~ 300 m/s x 10^{-6} s = 0.03 mm before it recombines.

- P8 L147, "the ions can form in a pure nitrogen environment almost like in the mentioned case of Wiedensohler and Fissan (1991)", what do you mean?

We will modify this sentence accordingly:
"As the working gas flow is exposed to a high frequency electrical field before it mixes with the aerosol flow, the ions can form in a pure nitrogen environment. Hence the charger ions form in a nitrogen atmosphere like in the case of Wiedensohler and Fissan (1991) where silver and sodium chloride particles were charged with a Kr 85 source in a pure nitrogen atmosphere. "

- Figure 5. It is not described how the normalization is done for the right hand side plot. It is hard to believe that the differences in the distributions are only due to charging. At 8-10 nm the charging efficiency of the X-ray is about 10 times larger than of the torch which is opposite to what is reported in Fig4. On the other hand, at 3 nm the torch shows charging efficiency of a factor of 5 higher than the X-ray, which is also contradictory to fig4.

At this point we want to mention that Figure 5 is rather a qualitative representation than a quantitative one, because of the rotated periodical measurements which were conducted in multiple cycles. The discussed shifts in the number concentration especially for the small sizes, for example 3 nm particles might also be a result of the temperature-fluctuations inside the tube furnace. Furthermore, the deviation at 8-10 nm for the X-Ray charger might be a result of the ammonium sulfate contaminations measured with the mass spec and by the ion mobility measurements where an increase of about 0.25 nm for the negative ions was found. The comparison of the mobility equivalent diameters from the classifier nDMA to the scanning nDMA did not show a significant difference for the 241Am neutralizer and the plasma torch.

We will change the following paragraph accordingly:
"Figure 5 depicts the recorded negatively charged aerosol size distribution averaged over numerous measurements, as well as the charging efficiency of the individual chargers normalized to the 241Am charger recordings. The normalization was done by comparing the recorded total number concentration of the individual neutralizers with the recorded total number concentration of the 241Am charger. The inversion of the size distribution data was performed according to Petters (2018). These diagrams permit a qualitative descriptive comparison of the different charging devices. The left plot reveals a shift of about 1 nm in the maximum of the recorded size distribution between the X-Ray and the plasma charger, which might be a result of small shifts in the size distribution originated from the tube furnace because of small temperature-fluctuations. Furthermore, contaminations of the X-Ray charger from previous experiments with ammonium sulfate might also lead to an increased particle diameter for the observed neutralizer (Steiner and Reischl, 2012)."

Furthermore, will change the Figure 5 caption:
"The plot on the left side represents the same recorded negative Ag aerosol size distribution with a UCPC, depending on the mobility diameter for the plasma torch (N2), X-Ray and americium neutralizers. On the right-hand side all conducted measurements with the same aerosol distribution are normalized to the 241Am results for a direct comparison."

- Figure 6, the intro discusses with one sentence the nT product. Is that product sufficient in the chargers to reach the steady state charge distribution?

According to the manufacturer the applied X-Ray neutralizer can be used for aerosol flow rates up to 5 L/Min and the 241Am charger used in this study was characterized by Kallinger et al. (2015) for flowrates up to 5 L/Min. Hence, we used the 241Am neutralizer as a reference which reaches steady state charge distributions and compared it the other measurements. The higher charging efficiency might be a result of the high ion concentrations of ~10^13/cc which can be achieved in a cold plasma (Kurake et al., 2016). That is approximately 6 orders of magnitude above the ion concentration inside a conventional Am241 aerosol charger (Steiner et al., 2014).

- P10 L185, ". The positive mass spectra were normalized to the nitrate ion (NO−3) peak at an integer mass of 62 Th and the negative mass spectra to the (H2O)2 H3O+ water cluster at an integer mass of 55 Th", the polarities do not match

We would like to thank the reviewer for making us aware, we will change it in the manuscript accordingly:

“The negative mass spectra were normalized to the nitrate ion (NO−3) peak at an integer mass of 62 Th and the positive mass spectra to the (H2O)2·H3O+ water cluster at an integer mass of 55 Th.”

- Section 2.1.3, previously there was discussion on the ionization of copper, why there is no copper signal in the charger ions?

Due to the low mean lifetime of this copper ions (about $1/(9 \times 10^6) \sim 0.1$ µs) it cannot be detected with the mass spec or with the UDMA setup.

- P12 L211, “(NH4)14SO− 4”, is it really a cluster of 14 NH4 ammonium molecules?

We will change the following sentence:
“According to our mass spec analysis, this is due to ammonium sulfate contaminations from previous experiments.”

- P15 L214, I would not say the are the same. Especially in positive there seem to be differences

We will reformulate this sentence:
“The presented measurements conducted with a non-thermal plasma source have shown that helium, nitrogen and air as working gases lead to the same ion species. According to the mobility and mass spec measurements the comparison of the plasma charger with the americium neutralizer indicates the same negative ion species. Whereas for the positive ions the measurements reveal a slight deviation.”

- P15 L218, it was shown nowhere that the torch produces ozone.

Preliminary measurements were already conducted with an ozone monitor which will be included in the manuscript to support the statement in the conclusion section.

- P15 L219, increased compared to what?

We will change the following sentence accordingly:
“By switching the working gas to nitrogen an increased charging efficiency could be recorded for negatively charged particles compared to 241Am neutralizer.”

References:

1) Barmpounis, K., A. Ranjithkumar, A. Schmidt-Ott, M. Attoui, and G. Biskos. Enhancing the detection efficiency of condensation particle counters for Sub-2nm particles. J. Aerosol Sci. 117 :44–53. doi: 10.1016/j.jaerosci.2017.12.005, 2018.
2) Sophia Brilke, Julian Resch, Markus Leiminger, Gerhard Steiner, Christian Tauber, Peter J. Wlasits & Paul M. Winkler. Precision characterization of three ultrafine condensation particle counters using singly charged salt clusters in the 1–4 nm size range generated by a bipolar electrospray source, Aerosol Science and Technology, 54:4, 396-409, DOI: 10.1080/02786826.2019.1708260, 2020.
3) William A. Hoppel & Glendon M. Frick. Ion—Aerosol Attachment Coefficients and the Steady-State Charge Distribution on Aerosols in a Bipolar Ion Environment, Aerosol Science and Technology, 5:1, 1-21, DOI: 10.1080/02786828608959073, 1986.

4) Kallinger, P. and Szymanski, W.: Experimental determination of the steady-state charging probabilities and particle size conservation in non-radioactive and radioactive bipolar aerosol chargers in the size range of 5–40 nm, Journal of Nanoparticle Research, 17,https://doi.org/10.1007/s11051-015-2981-x, 2015.
5) Kallinger, P., Steiner, G., and Szymanski, W.: Characterization of four different bipolar charging devices for nanoparticle charge conditioning, Journal of Nanoparticle Research, 14, https://doi.org/10.1007/s11051-012-0944-z, 2012.
6) Kramida, Alexander; Nave, Gillian; Reader, Joseph. The Cu II Spectrum. Atoms 5, no. 1: 9. doi:10.3390/atoms5010009, 2017.
7) Kurake N, Tanaka H, Ishikawa K.: Cell survival of glioblastoma grown in medium containing hydrogen peroxide and/or nitrite, or in plasma-activated medium. Arch Biochem Biophys. 605:102-108. doi:10.1016/j.abb.2016.01.011, 2016.
8) Petters, M. D.: A language to simplify computation of differential mobility analyzer response functions, Aerosol Science and Technology,52, 1437–1451, https://doi.org/10.1080/02786826.2018.1530724, 2018.
9) Reischl, G., Mäkelä, J., Karch, R., and Necid, J.: Bipolar charging of ultrafine particles in the size range below 10 nm, Journal of Aerosol Science, 27, 931 – 949, https://doi.org/https://doi.org/10.1016/0021-8502(96)00026-2, fuchs Memorial Issue, 1996.
10) Steiner, G. and Reischl, G. P.: The effect of carrier gas contaminants on the charging probability of aerosols under bipolar charging conditions, Journal of Aerosol Science, 54, 21 – 31, https://doi.org/https://doi.org/10.1016/j.jaerosci.2012.07.008, 2012.
11) Gerhard Steiner, Tuija Jokinen, Heikki Junninen, Mikko Sipilä, Tuukka Petäjä, Douglas Worsnop, Georg P. Reischl & Markku Kulmala: High-Resolution Mobility and Mass Spectrometry of Negative Ions Produced in a 241Am Aerosol Charger, Aerosol Science and Technology, 48:3, 261-270, DOI: 10.1080/02786826.2013.870327, 2014.
12) Tauber, C., Brilke, S., Wlasits, P., Bauer, P., Köberl, G., Steiner, G., and Winkler, P.: Humidity effects on the detection of soluble and insoluble nanoparticles in butanol operated condensation particle counters, Atmospheric Measurement Techniques, 12, 3659–3671,https://doi.org/10.5194/amt-12-3659-2019, 2019a.
13) Tauber, C., Steiner, G., and Winkler, P. M.: Counting efficiency determination from quantitative intercomparison be-tween expansion and laminar flow type condensation particle counter, Aerosol Science and Technology, 53, 344–354,https://doi.org/10.1080/02786826.2019.1568382, 2019b.
14) Tigges, L., Wiedensohler, A., Weinhold, K., Gandhi, J., and Schmid, H.-J.: Bipolar charge distribution of a soft X-ray diffusion charger, Jour-nal of Aerosol Science, 90, 77 – 86, https://doi.org/https://doi.org/10.1016/j.jaerosci.2015.07.002, 2015.
15) Wiedensohler, A.: An approximation of the bipolar charge distribution for particles in the submicron size range, Journal of Aerosol Science, 19, 387 – 389, https://doi.org/https://doi.org/10.1016/0021-8502(88)90278-9, 1988.
16) Wiedensohler, A. and Fissan, H. J.: Bipolar Charge Distributions of Aerosol Particles in High-Purity Argon and Nitrogen, Aerosol Science and Technology, 14, 358–364, https://doi.org/10.1080/02786829108959498, 1991.
17) Wiedensohler, A., Lütkemeier, E., Feldpausch, M., and Helsper, C.: Investigation of the bipolar charge distribution at various gas conditions, Journal of Aerosol Science, 17, 413 – 416, https://doi.org/https://doi.org/10.1016/0021-8502(86)90118-7, 1986.

18) Winkler, P. M., G. Steiner, A. Vrtala, H. Vehkamäki, M. Noppel, K. E. J. Lehtinen, G. P. Reischl, P. E. Wagner, and M. Kulmala. Heterogeneous nucleation experiments bridging the scale from molecular ion clusters to nanoparticles. Science 319 (5868):1374–1377. doi: 10.1126/science.1149034, 2008.

We appreciate the thoughtful comments by referee #2. For discussion purposes we would like to respond to the general and detailed points raised.

This work describes the use of a plasma torch as an aerosol neutralizer. The work measures and compares the charging probability of the new source with commercial available other aerosol chargers. The charging probabilities were measured for positive and negative particles (Ag, and NaCl) and at different aerosol flow rates. In addition, the plasma torch has been evaluated at operation with different working fluids (He, Ar, N2). The mobility distributions and mass graphs of the charger ions were also measured in order to get an information on the properties of the charger ions. The work includes a very thorough investigation of the charger source and the charger ions. However, there are a few general concerns about the work, that should be addressed before publication:

1. The plasma torch itself, is not described at all in the current manuscript, a paragraph on the working principle should be added to the manuscript.

There is indeed not much information given about the charger itself and we acknowledge that this is unusual for a research paper. However, we have to point out that there is still a patent pending and, thus, we cannot reveal all the technical details of how the charger works. Broadly speaking the atmospheric pressure plasma charger consists of a gas flow that is shielded by another gas flow from the surrounding atmosphere. The plasma is ignited inside the inner flow while the aerosol is administered through the outer gas stream. The main source of the plasma is a high-frequency copper electrode that is situated on the central axis of those two gas streams.

We will add the following description to the experimental section:
"The atmospheric pressure plasma charger consists of a gas flow that is shielded by another gas flow from the surrounding atmosphere. The plasma is ignited inside the inner flow while the aerosol is administered through the outer gas stream. The main source of the plasma is a high-frequency copper electrode that is situated on the central axis of those two gas streams."

2. In the measurement with different gases, one would expect that using a DMA and CPC in a helium-air mixture would result into changes in the instrument performance. The voltage mobility relationship in the DMA is gas dependent, and in the CPC the flow calibration would change when adding helium to the system, also the supersaturation profile would change and the detection limit would shift to smaller particles (e.g. Thomas et al. 2018, Journal of Heat and Mass Transfer). These are points that should be addressed in this manuscript.

We will add the following statement to the manuscript:
"The additional flow rate from the working gas was at max 1/9 of the aerosol flow. According to Thomas et al. (2018) a cutoff drift to lower sizes for helium mole fractions below 0.67 was found for butanol-based CPCs. However, the used CPC in this study was operated with reduced temperature settings and thereby a lower detection efficiency was established (Tauber et al. 2019a). As a result, the recorded cutoff drift would therefore only influence the charging efficiency measurements conducted at < 3 nm. The resulting error is already covered for this particle sizes by the measurement uncertainties of nDMA and CPC."

3. The charger ion mass and mobilities were measured, however, no qualitative thoughts were included in how and why that would result into the observed changes of charging probability. It has been stated correctly that the charger ion composition plays an important role to the final charge distribution. But what is missing is to apply the information found in this work to existing theories and see if the trend agrees with the observations. Simulation results of charge distributions considering different ion mass and mobility of charger ions have been performed in the past, see for example Maisser et al, 2015, Journal of Aerosol Science

We compared our results to approximations given by Wiedensohler (1988) and Tigges et al. (2015) and performed calculations for different ion masses and mobilities. The results of the calculations are posted in the review comment #1 and will be added to the manuscript.

4. The results of the optical emission spectroscopy seem very isolated from the rest of the publication. It is not clear how these experiments were performed. This is a bit confusing, is this supposed to be part of the experimental setup description, or already an experimental results section? If it is experimental results, then the procedure of how these measurements were done should be added in a bit more detail in the experimental section. Was this a completely separate measurement, or did you do that while aerosol generation and charging was happening as well? This would require also a description of the source itself, which was already mentioned above. Was the optical emission spectroscopy done only in pure helium environment, and how would that be relevant to the rest of the measurement?

The optical emission spectroscopy was conducted as a separate experiment with the flow rates stated in the supplemental material but without aerosol generation. The emission spectra yield additional information about the charging mechanism and the plasma itself. The former encompasses the discovery that the charging of the aerosol particles is achieved via electrons that originate from the central electrode of the charger. The latter point includes, for example, the detection of singly charged He particles, which have a lifetime that is so short that they recombine before reaching the detector in the ioniAPi-TOF. Furthermore, the OES measurements led to a better understanding of the plasma behavior and, thus, the way of charge transfer from the plasma to the molecules or aerosols. The electrons are detached from the high-frequency copper electrode as those atoms are easily ionized. After leaving the electrode the charges attach themselves onto preexisting molecules or aerosol particles. As a result, based on the ioniAPi-TOF and mobility measurements it was shown that the different charging mechanism lead to comparable measurement results.

We will add the following to the experimental section:
“The optical emission spectrometer was located at the nozzle of the plasma charger and used to record spatially averaged optical data along the axis of the plasma source.”

Some more detailed comments:
Ad Section 2) Experimental Setup: No description, schematic or anything on the charger!

We will add the following description to the experimental section:
“The atmospheric pressure plasma charger consists of a gas flow that is shielded by another gas flow from the surrounding atmosphere. The plasma is ignited inside the inner flow while the

aerosol is administered through the outer gas stream. The main source of the plasma is a high-frequency copper electrode that is situated on the central axis of those two gas streams.
According to Kallinger et al. (2012), the used radioactive 241Am charger has a cylindrical geometry with an axial flow direction. The radioactive source is mounted on the inner wall. The chamber has an inner diameter of about 30 mm and a length of 120 mm. Furthermore, the soft x-ray charger is composed of a stainless-steel tube and a photo ionizer. The aerosol particles are directed along the tube towards the soft x-ray source and leave the charger via an outlet, that is oriented perpendicularly to the axis of the tube. The tube has an inner diameter of 30 mm and a length of 200 mm."

Page, Fig. 2: It seems like the mobility distributions were measured in an air Helium, Argon, or N2 mixture. But I don't see any discussion of the influence of this gas mixture on the mobility measurements. If the DMA has been operated in a closed loop this has to be considered. The mobility of THAB in a helium air mixture would not be the same, so how was the calibration done in this case? If this was considered and found to be negligible a discussion and reference has to be added. If it has not been considered, then this needs to be done.

The mobility distributions were measured with air as carrier gas and only for the plasma charger an additional working gas (Air, N2, He) was added. This working gas flow was between 40 and 280 cc/min. The mobility spectrum / calibration measurement with THAB was always recorded with air as carrier gas. After the calibration the charger was mounted to the setup and the experiments with different working gases was conducted. So, there was no helium air mixtures during the calibration runs in the sheath air of the UDMA.

Section 2.1. I think this should be numbered 3, not 2.1, since it does not seem to be part of the experimental setup

Thank you for making us aware of the wrong numbering. We will separate the results and discussion section from the experimental section.

Page 5, line 94, 95: What is the copper antenna for?

We will add the following sentences on P5 L89 to explain the antenna and its usage:
"Thereby the plasma jet is shielded by another gas flow from the surrounding atmosphere. The plasma is ignited inside the inner flow while the aerosol is administered through the outer gas stream. The main source of the plasma is a high-frequency copper antenna/electrode that is situated on the central axis of those two gas streams."

Page 8, line 144 says that the different masses of charger ions created in the plasma torch and the other charger sources might result in the observed differences. Can this be quantified. Is the mean mass, and mobility higher or larger than in the other case. How does an increase or decrease of mass and mobility affect the final result. Why did you not apply the measured mass and mobility to the theory?

We would like to thank the reviewer for his thoughtful comments and make him aware of the performed calculations for different ion masses and mobilities which are posted in the review comment #1 and which will be added to the manuscript.

Page 9, line 163, why would it charge better in air than in helium? And how can the large difference of 50% be explained?

We will add the following paragraph to the manuscript:
"According to Maisser et al. (2015), nitric acid has an anomalously high gas phase acidity for its mass and can persist in the gas phase in higher concentrations than other low mass species. By using helium as working gas the concentration of nitrate ions in the gas phase is lower than in air or N2 and therefore charge transport decreases. This is contrary to using N2 as working gas where an increased charging efficiency up to 50% was measured."

Page 10, line 185, polarities wrong, also, you should mention that it was the y-axis that was normalized

We will change it in the manuscript accordingly:
"The negative mass spectra were normalized to the nitrate ion (NO^-_3) peak at an integer mass of 62 Th and the positive mass spectra to the $(H2O)2{\cdot}H3O^+$ water cluster at an integer mass of 55 Th."

Page 11, Fig. 7, for negative mass graphs the chemical equations are mentioned but not the mass, while for the positive ions it's the other way around. Is there a reason for that? What are the rectangles in the positive Am-241?

The dashed square box marks unidentified masses in the positive 241Am mass spectrum and the solid square box shows the silicone compounds that are listed in Table 2 in the Manuscript. For space reason we mentioned only the chemical equations for the negative masses but in Table 3 all chemical equations and masses are listed.

References:

1. Kallinger, P., Steiner, G., and Szymanski, W.: Characterization of four different bipolar charging devices for nanoparticle charge conditioning, Journal of Nanoparticle Research, 14, https://doi.org/10.1007/s11051-012-0944-z, 2012.
2. Maisser, A., Thomas, J. M., Larriba-Andaluz, C., He, S., & Hogan, C. J., The mass-mobility distributions of ions produced by a Po-210 source in air. Journal of Aerosol Science, 90, 36-50. https://doi.org/10.1016/j.jaerosci.2015.08.004, 2015.
3. Tauber, C., Steiner, G., and Winkler, P. M.: Counting efficiency determination from quantitative intercomparison be-tween expansion and laminar flow type condensation particle counter, Aerosol Science and Technology, 53, 344–354,https://doi.org/10.1080/02786826.2019.1568382, 2019a.

4. Jikku M. Thomas and Xiaoshuang Chen and Anne Maißer and Christopher J. Hogan, Differential heat and mass transfer rate influences on the activation efficiency of laminar flow condensation particle counters. International Journal of Heat and Mass Transfer, 127, 740-750. https://doi.org/10.1016/j.ijheatmasstransfer.2018.07.002, 2018.
5. Tigges, L., Wiedensohler, A., Weinhold, K., Gandhi, J., and Schmid, H.-J.: Bipolar charge distribution of a soft X-ray diffusion charger, Jour-nal of Aerosol Science, 90, 77-86, https://doi.org/https://doi.org/10.1016/j.jaerosci.2015.07.002, 2015.
6. Wiedensohler, A.: An approximation of the bipolar charge distribution for particles in the submicron size range, Journal of Aerosol Science, 19, 387 – 389, https://doi.org/https://doi.org/10.1016/0021-8502(88)90278-9, 1988.

Characterization of a Non-Thermal Plasma Source for the Use as a Mass Spec Calibration Tool and Non-Radioactive Aerosol Charger

Christian Tauber[1], David Schmoll[1], Johannes Gruenwald[2], Sophia Brilke[1], Peter Josef Wlasits[1], Paul Martin Winkler[1], and Daniela Wimmer[1]

[1]Faculty of Physics, University of Vienna, Boltzmanngasse 5, 1090 Vienna, Austria
[2]Gruenwald Laboratories GmbH, Taxberg 50, 5660 Taxenbach, Austria

Correspondence: Christian Tauber (christian.tauber@univie.ac.at)

Abstract. In this study the charging efficiency of a radioactive and a non-radioactive plasma neutralizer (Gilbert Mark I plasma charger) have been investigated at various aerosol flow rates. The results were compared to classic theoretical approaches. In addition, the chemical composition and electrical mobilities of the charger ions have been examined using an atmospheric pressure interface - time-of-flight mass spectrometer (APi-TOF MS). A comparison of the different neutralization methods revealed an increased charging efficiency for negatively charged particles using the non-radioactive plasma charger with nitrogen as working gas compared to a radioactive americium neutralizer. The mobility and mass spectrometric measurements show that the generated neutralizer ions are of the same mobilities and composition independent of the ~~charging mechanism~~examined neutralizer. It was the first time that the Gilbert Mark I plasma charger was characterized in comparison to ~~the standard~~ a commercial TSI X-Ray (TSI Inc, Model 3088) and a radioactive americium neutralizer. We observed that the plasma charger with nitrogen as working gas can enhance the charging probability for sub-10 nm particles compared to a radioactive americium neutralizer. Consequently, the limit of detection of differential or scanning mobility particle sizers can be increased ~~down towards to smaller sizes~~ to nanometer sized particles with the Gilbert Mark I plasma charger.

1 Introduction

Bipolar diffusion charging and neutralization is typically done by ionizing radiation, which exposes aerosol particles to high concentrations of positive and negative ions in the carrier gas (Jiang et al., 2014). Subsequent diffusion of the ions brings the aerosol to a stationary state charge distribution independent of their initial charge state (Cooper and Reist, 1973; Liu and Pui, 1974; Adachi et al., 1985; Reischl et al., 1996). If a high ion concentration and residence time is reached, a charge equilibrium inside the charger leads to a well known size-dependent charging probability (Fuchs et al., 1965). This stationary state charge distribution is of importance for the use of differential or scanning mobility particle spectrometers, which rely on accurate knowledge of the size-dependent charge fractions (Wang and Flagan, 1990; Jiang et al., 2014). Aerosol particles below 10 nm in diameter are typically difficult to ~~neutralize~~ charge and carry only one electrical charge at maximum (Wiedensohler, 1988). Quantitative particle detection in this size range is extremely challenging due to high diffusional losses~~. Hence~~, which results in low number concentrations. Therefore, a higher charging efficiency is of importance to ~~improve the signal intensity~~ increase

the detectable number concentration in the sub-10 nm regime.

The charging of small particles has also become a field of major interest in plasma physics. A vast number of studies about accumulating an electrical charge on dust particles have been published over the last years. Usually grain sizes ranging from some nm to several μm are considered in the experiments and theoretical models. Most of these works were focused on generating plasmas for industrial or space applications (Michau et al., 2016; Deka et al., 2017; Kopnin et al., 2018; Yaroshenko et al., 2018; Intra and Yawootti, 2019). However, one of the most recent developments is the application of plasma in aerosol related topics, such as plasma treatment of aerosol particles (Uner and Thimsen, 2017) and, as a novel topic, charging of aerosol particles or ionization of trace gas compounds (Spencer et al., 2015; Yang et al., 2016; Intra and Yawootti, 2019). Usually, corona-type discharges are used for the charging purposes in aerosol physics due to their capability of creating high charge densities even at atmospheric pressure. Furthermore, their reproducibility is very high and they are easy to construct and maintain. Low-temperature plasma ionization is known to cause little fragmentation and exhibits a low temperature increase to the surrounding (Harper et al., 2008). The non-thermal plasma in this work is produced by a high frequency generator which is separated by a dielectric barrier to the ground potential (Gruenwald et al., 2015). The ~~discharge~~ term non-thermal plasma is usually used to describe a discharge in which the electrons are in thermal non-equilibrium with the ions. This means that the average temperature of the gas in such a discharge is far lower than the temperature of a thermal plasma (i.e. some hundred K compared to several thousand K in the latter case). The discharge characteristics can be varied by changing the working gas of the Gilbert Mark I plasma charger (Gruenwald Laboratories GmbH). Plasma discharges in general are on-off devices that combine the simple handling of an X-ray charger with the achievable high ion density of a radioactive americium charger and even higher. Thus, an atmospheric plasma source is a well-suited device for the ionization process prior to aerosol size distribution measurements and mass spectrometric measurements.

In the past, various studies have characterized the charging probabilities and mobility ~~spectrum of~~ spectra of the charger ions produced by AC-corona, X-Ray or alpha-radiation based chargers (Wiedensohler et al., 1986; Steiner and Reischl, 2012; Kallinger et al., 2012; Kallinger and Szymanski, 2015). In this work, we present the experimental results obtained with the commercially available Gilbert Mark I plasma charger, which will be described in more detail in the next section. In addition, the chemical composition of charger ions of both polarities has been investigated and compared. Furthermore, the optical emission spectra and ozone concentration were measured for the Gilbert Mark I plasma charger.

2 Experimental Setup

Here we report on size-dependent ~~steady-state~~ charging probability measurements of a non-thermal plasma source (Gilbert Mark I plasma charger, Gruenwald Laboratories GmbH, Austria), an americium 241 (^{241}Am) charger and of a TSI Advanced Aerosol Neutralizer 3088 by means of a tandem DMA (Differential Mobility Analyzer) setup as depicted in Figure 1. Thereby, the charging efficiency of a standard TSI X-Ray neutralizer and an ^{241}Am charger could be compared to the plasma source. The atmospheric pressure plasma charger consists of a gas flow that is shielded by another gas flow from the surrounding atmosphere. The plasma is ignited inside the inner flow while the aerosol is administered through the outer gas stream. The

Table 1. Flow rates for the aerosol and sheath flow for the used nDMAs with the calculated sheath flow ratio.

nDMA	Aerosol flow [L/Min]	Sheath flow [L/Min]	Ratio
1	3.0	19.5	6.5
2	2.5	19.5	7.8
2	5.0	33.0	6.6
2	8.0	41.0	5.1

main source of the plasma is a high-frequency copper electrode that is situated on the central axis of those two gas streams. According to Kallinger et al. (2012), the used radioactive ^{241}Am charger has a cylindrical geometry with an axial flow direction. The radioactive source is mounted on the inner wall. The chamber has an inner diameter of about 30 mm and a length of 120 mm. Furthermore, the soft x-ray charger is composed of a stainless-steel tube and a photo ionizer. The aerosol particles are directed along the tube towards the soft x-ray source and leave the charger via an outlet, that is oriented perpendicularly to the axis of the tube. The tube has an inner diameter of 30 mm and a length of 200 mm.

The charging efficiency measurements were performed with sodium chloride and silver nanoparticles at various particle sizes and aerosol flowrates. The nanoparticles were generated with a tube furnace (Carbolite Gero GmbH & Co. KG, Germany) while synthetic air as well as dried and filtered compressed air were used as the carrier gas. An additional dilution flow allowed for controlling the particle concentration of the generated aerosol flow. Downstream of the aerosol generator the nanoparticles were charged with a TSI Advanced Aerosol Neutralizer 3088 and led to a ~~nanoDMA~~ nDMA which was operated as a classifier. A second TSI Advanced Aerosol Neutralizer 3088 neutralized the monodisperse aerosol particles after the ~~nanoDMA.~~ nDMA. The geometric standard deviation of the particle size for the used nDMAs was evaluated by Winkler et al. (2008) for a sheath flow of 25 L/Min and an aerosol flow of 4.6 L/Min and is below 1.05 for particles with a mobility diameter down to 2 nm. The resulting flow ratio (sheath / aerosol = 5.4) is close to our measurement with 8 L/Min aerosol flow and the signal-to-noise ratio was comparable to the measurements with lower aerosol flow rates. The different flow settings for the nDMAs are listed in Table 1.

To secure that no charged particles remain in the aerosol flow an ion-trap was installed after the neutralizer (Brilke et al., 2020) . After the ion-trap the aerosol flow was split in a way that 1.5 ~~lpm~~ L/Min were led to a CPC (TSI 3776 UCPC) which recorded the particle concentration at this point while the remaining aerosol flow was fed into the aerosol neutralizer under investigation. A dilution flow of synthetic air as well as compressed air allows for varying the flowrate before the aerosol flow gets to the neutralizer. The investigated neutralizers were switched in intervals of 10 minutes during the measurements to secure that the different devices were operated at comparable conditions. Afterwards the charged aerosol flow was led to a second ~~nanoDMA~~nDMA, which was operated in scanning mode. A second CPC (TSI 3776 UCPC) recorded the particle concentration at this point of the setup. In addition to the switching of the different neutralizers, the working gas as well as the working gas flow of the atmospheric pressure plasma source were varied.

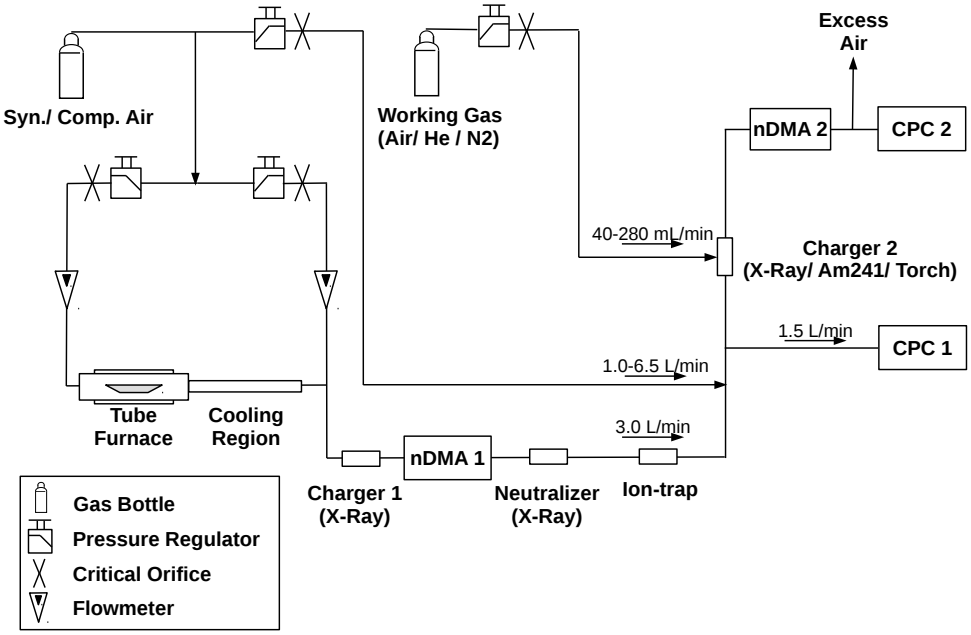

Figure 1. Schematic of the experimental setup for the charging probability and particle size conservation measurements. The additional working gas flow is only needed for the plasma charger. See text for explanation.

Complementary to the charging efficiency, the chemical composition of the charger ions were investigated by coupling the plasma torch with an APi-TOF MS (Atmospheric Pressure Interface - Time of Flight Mass Spectrometer, Junninen et al. (2010); Leiminger et al. (2019), see upper panel in Figure 2), to analyze the chemical composition of the ions generated in positive and negative ion mode. Mobility spectra were recorded with a custom-built Faraday Cup Electrometer (FCE) (Winklmayr et al., 1991) with an improved response time of 0.1 s. By recording the ion spectrum with a Vienna-type high-resolution mobility analyzer (UDMA-1, Steiner et al. (2010)), the mobility equivalent diameter of the generated clusters could be analysed (see lower panel in Figure 2). Compressed filtered and dry air was used as carrier gas and the relative humidity (RH) was monitored using SHT75 RH sensors with an accuracy of $\pm 1.8\%$ and was kept below 2%. However, we can not exclude that in the closed loop sheath flow system of the UDMA-1 small amounts of water vapor remain. The calibration of the ioniAPi-TOF mass axis was performed using a bipolar electrospray source for the generation of tetra-heptyl ammonium bromide clusters (Fernández de la Mora and Barrios-Collado, 2017; Brilke et al., 2020). The UDMA-1 resolution power is 15 at the size of the THABr monomer, i.e. 1.45 nm mobility equivalent diameter (Flagan, 1999; Steiner et al., 2010). Due to the high ion concentration of a non-thermal plasma source a vast number of reactive species are created, especially when the plasma is ignited in air (Kurake et al., 2016). Most of these species will be ozone or nitrogen oxides because of the air's chemical composition. Hence, the optical emission spectra of the non-thermal plasma source were recorded, which is a non-invasive diagnostic technique that

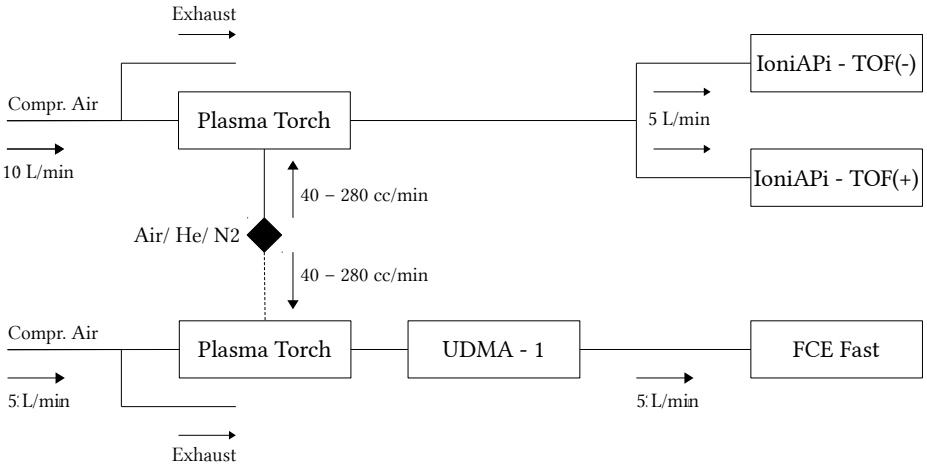

Figure 2. Schematic of the calibration setup for the plasma torch using an UDMA. The black rhombus marks the working gas supply. Mass spectra of negative and positive ions were measured simultaneously using the ioniAPi-TOF in negative and positive ion mode at a flow rate of 10 L/min through the plasma torch (upper panel) for the three working gases and operational settings. The mobility spectra of the generated positive and negative ions were measured using the UDMA-1 (Steiner et al., 2010) coupled to a fast-response FCE at 5 L/min flow rate.

allows to gain insights into the composition of the plasma and the production of harmful gases like ozone and nitrogen oxides. The optical emission spectrometer was located at the nozzle of the plasma charger and used to record spatially averaged optical data along the axis of the plasma source.

2.1 ~~Results and Discussion~~

3 Results and Discussion

3.0.1 ~~Optical Emission Spectroscopy~~

3.1 Optical Emission Spectroscopy

Optical emission spectroscopy (OES) was used to determine the ionization stages of the ions/molecules in the plasma. The measurements were performed with the HR2000+ES spectrometer from Ocean Optics. The light emission from the atmospheric pressure plasma source was collected with a 440 μm fiber with a length of 2 m. The wavelength range of the spectrometer was between 200 and 1100 nm. Prior to the data acquisition the torch was switched on for about 30 seconds until no fluctuations in the spectra were visible. Each spectrum is the result of averaging over 50 scans to remove fluctuations. The plasma source itself was driven with a high frequent alternate current of 15 kHz with 825 V peak-to-peak voltage. The plasma was ignited in helium of high purity (ALPHAGAZ 1 HELIUM, $>= 99.999\%$ (5.0), Air Liquide), which was fed into the plasma jet with a flow rate of 180 mL/min. The plasma is ignited inside the inner flow while the aerosol is administered through the outer gas

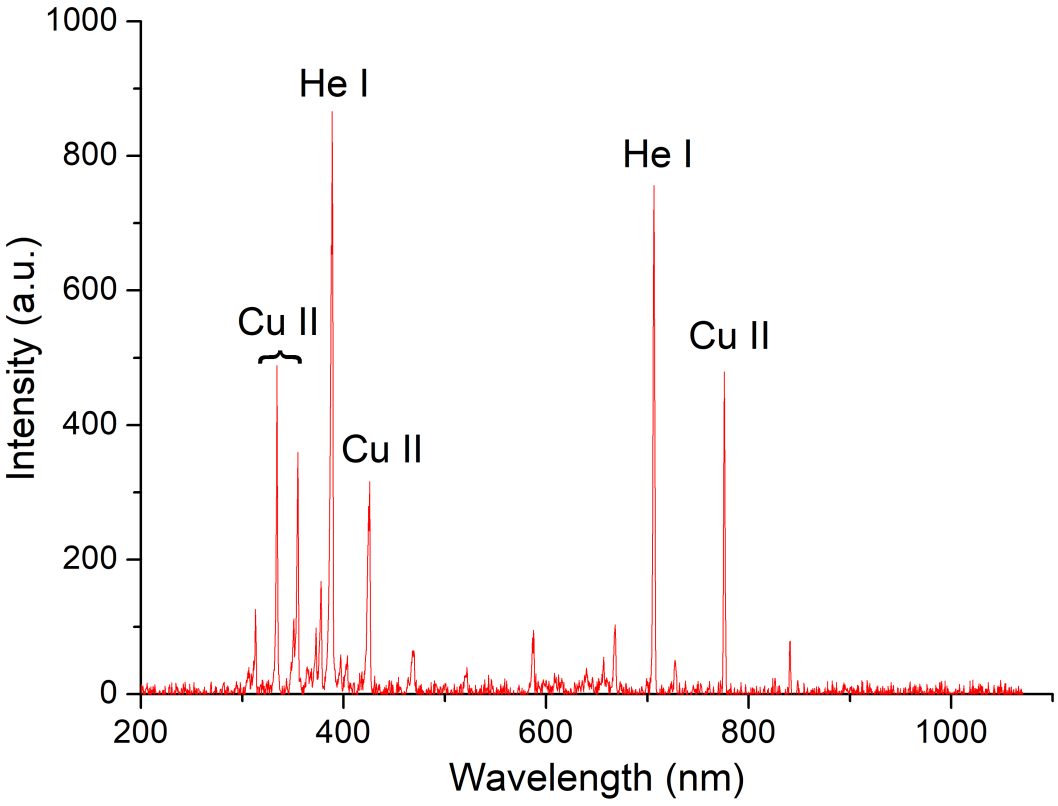

Figure 3. Typical OES spectrum in a helium plasma averaged over 50 scans. Experimental conditions: 15 kHz driving frequency, 825 volts peak-to-peak and 180 mL/Min He flow.

stream. The main source of the plasma is a high-frequency copper antenna/electrode that is situated on the central axis of those two gas streams. The results for a typical OES spectrum for the described experimental conditions are depicted in Figure 3.

The most prominent emission lines were identified to be excited neutral helium (He I) and singly ionized copper (Cu II). The central wavelengths of the identified lines are listed in Table 2.

It can be concluded from the OES spectra that there is no ionization of aerosol particles facilitated by the carrier gas, since only neutral helium emission lines have been recorded. On the other hand, atoms from the copper high frequency antenna enter the plasma zone and are then ionized through electron impacts. The charged particles created from these processes (i.e. ions and secondary electrons), in turn, charge the aerosol particles in the gas stream. This can be explained by the large difference in ionization energies between copper (7.7 eV) and helium (24.6 eV). Since the electrons in non-thermal atmospheric pressure discharges have normally energies of just a few eV, the ionization of copper atoms is far more likely than of helium particles.

Table 2. Measured Central wavelengths compared to data from Kramida et al. (2013) and the associated particle species for the most prominent emission lines in Figure 3.

Measured central wavelength [nm]	Wavelength from Kramida et al. (2013) [nm]	Particle Species
334.38	334.4	Cu II
354.86	354.9	Cu II
388.86	388.9	He I
425.67	425.6	Cu II
706.05	706.5	He I
755.56	775.4	Cu II

3.1.1 ~~Charging Probability~~

3.2 Charger ion chemical composition

~~The neutralizers~~

The ion properties of ionic molecular clusters produced in the plasma torch were investigated by means of electrical mobility and mass spectrometry. Mobility spectra and mass spectra were recorded for positive and negative ions and compared to the resulting spectra from ions produced in the $^{241}\mathrm{Am}$ charger. Figure 4 shows the mass spectra for negative (left) and positive (right) ions generated by the $^{241}\mathrm{Am}$ charger (first panel) and the plasma torch for the three different working gases (second to fourth panel) using the setups shown in Figure 2 at the working gas flow settings presented in Table S1 and S2 in the supporting information (SI). The negative mass spectra were normalized to the nitrate ion (NO_3^-) peak at an integer mass of 62 Th and the positive mass spectra to the $(H_2O)_2 \cdot H_3O^+$ water cluster at an integer mass of 55 Th. The negative mass spectra are dominated by the nitrate ion, NO_3^-, and its dimer, trimer and water cluster (see labels in second panel in Figure 4). The three spectra for charger ions produced from the torch exhibit the same major peaks with the nitrate ion trimer peak being highest when He is used as working gas (see fourth panel). This observation may be a result of the different operational settings of the plasma torch when He is used as working gas (see Table S1 and S2). The negative ion spectrum of the $^{241}\mathrm{Am}$ charger reveals the same major peaks as the plasma torch negative mass spectra. Similar results have been found by a study investigating the chemical composition of ions produced by a corona discharge (Manninen et al., 2011). The identified major peaks of the positive mass spectra are listed in Table 3. In the lower mass range between 40 - 80 Th, protonated water, H_3O^+, and water clusters thereof dominate the spectrum for the $^{241}\mathrm{Am}$ charger and the three spectra of the plasma torch. The elemental composition of four major peaks in the positive spectra of the plasma torch at integer masses of 88, 175, 187 and 201 Th were identified as carbonaceous compounds. In the higher mass range between 600 - 1000 Th, a set of major peaks was identified as silicone compounds. The same peaks were identified in the positive mass spectra of ions produced from the $^{241}\mathrm{Am}$ charger (solid black box in Figure 4). This observation was also made by Manninen et al. (2011), who explain these peaks as a result of contamination from silicone tubing. Silicone tubing is oftentimes used in aerosol measurements and can cause artifacts because

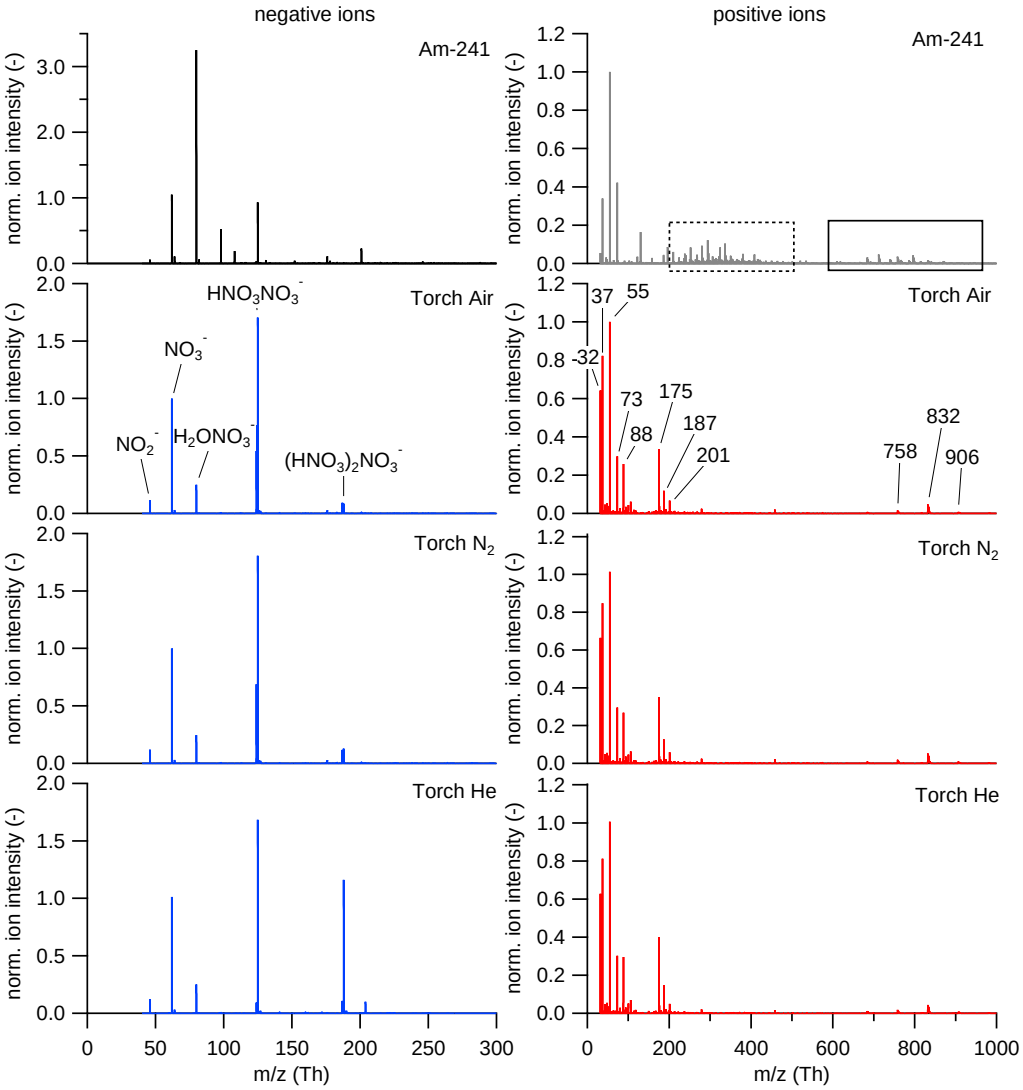

Figure 4. Negative (left) and positive (right) mass spectra of ions generated by the ^{241}Am charger (first panel) and the plasma source for three different working gases, synthetic air (second panel), N_2 (third panel) and He (fourth panel) were measured using the setup in the upper panel of Figure 2. The mass spectra were averaged over 1 hour each. The identified compounds are labeled in the second panel and are presented in Table 3. The negative mass spectrum was normalized to the NO_3^- ion (integer mass 62 Th), the positive mass spectrum was normalized to the $(H_2O)_2 \cdot H_3O^+$ cluster (integer mass 55 Th). The H_3O^+ ion is not displayed here since it was not covered by the set mass range of the ioniAPi-TOF. The dashed square box marks unidentified masses in the positive ^{241}Am mass spectrum and the solid square box shows the silicone compounds that are listed in Table 3.

of degassing of siloxanes (Asbach et al., 2016). However, a range of peaks in the mass window from approximately 200 to 500

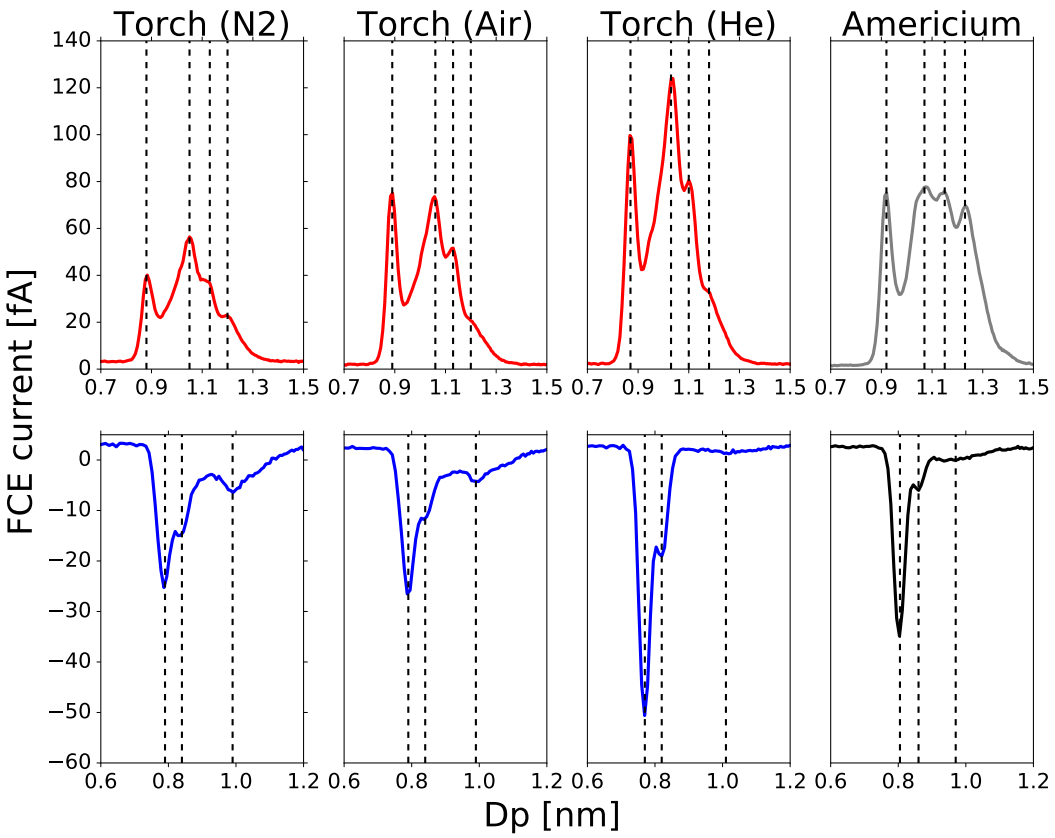

Figure 5. Mobility distributions of the charger ions generated by the plasma torch using N_2, He and air as working gas and the ^{241}Am charger. The upper panel shows the mobility diameter distribution of the positive charger ions, the lower panel presents the mobility diameter distribution of the negative charger ions.

Th remains unidentified (dashed black box). These carbonaceous compounds have a positive mass defect and likely arise from ionization of constituents in the pressurized air that was used as carrier gas.

The chemical composition of the plasma-generated ions was found to be independent of the choice of the working gas as shown in Figure 4. Also, the averaged electrical mobility measurements (averaged over 10 scans) conducted with the experimental setup depicted in Figure 2 (lower panel) revealed identical peaks. The mobility spectra for the plasma torch using N_2, He and air as working gas and the ^{241}Am charger are presented in Figure 5. Similar results for different bipolar charging devices have been found by Kallinger et al. (2012) and Steiner and Reischl (2012). The latter have analysed the effects of carrier gas contaminants on the charging probability which influences the electrical mobility spectrum. One of the analysed TSI X-Ray charger showed a different mobility spectrum compared to the other analysed neutralizers. According to our mass spec analysis, this is due to ammonium sulfate contaminations from previous experiments.

Table 3. Overview of major negative and positive compounds in the mass spectra recorded using the ioniAPi-TOF in positive and negative ion mode.

Negative Ions		Positive Ions	
Integer m/z (Th)	Molecular Formula	Integer m/z (Th)	Molecular Formula
46	NO_2^-	32	O_2+
62	NO_3^-	37	$H_2O \cdot H_3O^+$
80	$H_2O \cdot NO_3^-$	55	$(H_2O)_2 \cdot H_3O^+$
124	-	73	$(H_2O)_3 \cdot H_3O^+$
125	$HNO_3 \cdot NO_3^-$	88	$C_4H_{10}NO^+$
187	-	175	$C_4H_9NO \cdot C_4H_{10}NO^+$
188	$(HNO_3)_2 \cdot NO_3^-$	187	$C_{10}H_{21}NO_2^+$
		201	$C_{11}H_{23}NO_2^+$
		610	$(SiOC_2H_6)_8OH_2^+$
		684	$(SiOC_2H_6)_9OH_2^+$
		758	$(SiOC_2H_6)_{10}OH_2^+$
		832	$(SiOC_2H_6)_{11}OH_2^+$
		906	$(SiOC_2H_6)_{12}OH_2^+$

3.3 Charging Probability

The neutralizers were tested in the setup shown in Figure 1, in order to characterize the charging performance of the plasma torch (Gilbert Mark I plasma charger) and the ^{241}Am as well as the soft X-Ray charger. The tandem DMA setup enabled us to charge a monodisperse aerosol and rotate the different neutralizers, which permits a direct comparison of the charging performance of the different devices. Two butanol-based CPCs (TSI 3776 UCPC) with reduced temperature settings ~~to~~ (Condenser 1.1°C, Saturator 30.1°C, Optics 31.1°C) compared to factory settings to increase the particle counting efficiency were used ~~(Tauber et al., 2019a)~~(Barmpounis et al., 2018; Tauber et al., 2019a). The particle number concentration was recorded before (CPC1, See Fig. 1) and after charging (CPC2) by the tested charger (Charger 2). The charging efficiency was inferred from the ratio of the two CPCs (CPC2/CPC1) under consideration of the transmission and diffusional particle losses in the lines and DMA. In Tauber et al. (2019b) the particle counting efficiency of the CPCs used here was determined, and the results obtained were used to corrected for the CPC detection efficiency. The different neutralizers were tested with positively and negatively charged Ag and NaCl particles of different particle sizes in the ~~sub-10~~ sub-15 nm regime. In addition, the plasma torch was operated with different working gases. The additional flow rate from the working gas was at max 1/9 of the aerosol flow. According to Thomas et al. (2018) a cutoff drift to lower sizes for helium mole fractions below 0.67 was found for butanol-based CPCs. However, the used CPC in this study was operated with reduced temperature settings and thereby a lower detection efficiency was established. As a result, the recorded cutoff drift would therefore only influence the charging efficiency measurements

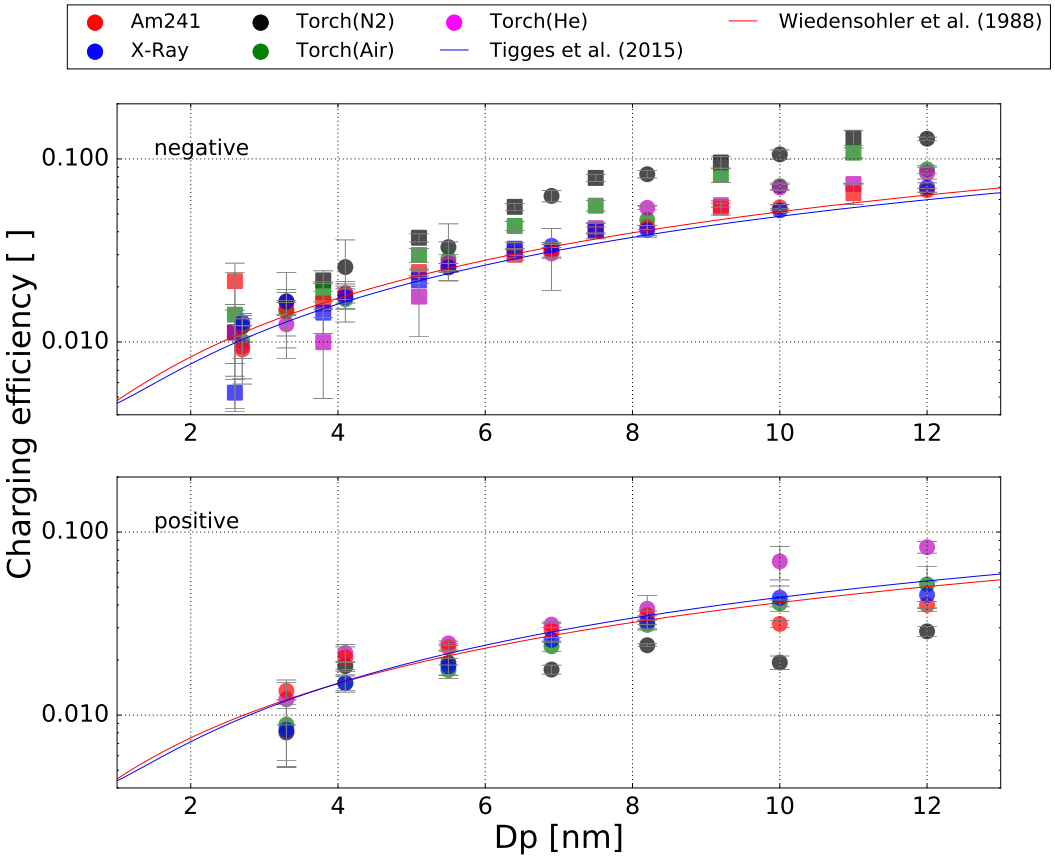

Figure 6. Measured charging efficiencies for the different aerosol chargers for negatively and positively charged Ag particles (dots) and negatively charged NaCl particles (squares) with mobility diameters less than 12 nm.

conducted at < 3 nm. The resulting error is already covered for this particle sizes by the measurement uncertainties of the nDMA and CPC.

The results of the charging efficiency when using the three different working gases are displayed in Figure 6. Theoretical charging probabilities from Tigges et al. (2015) and Wiedensohler (1988) were added here.

Concerning negatively charged particles with a diameter between 4-12 nm the ^{241}Am and the soft X-Ray charger are in agreement with the theoretical curves especially with Wiedensohler (1988). The plasma torch on the other hand achieves higher charging efficiencies in this regime with big differences between the used working gases. With helium the charging efficiencies were higher than the theoretical values, especially for particle sizes bigger than 8 nm. Ambient air yields even higher charging probabilities but displays a significant dependency on the particle type as the values for NaCl particles are a lot higher than for Ag particles. The highest charging efficiencies for negatively charged particles were achieved with nitrogen as working gas. With nitrogen the plasma torch achieved charging efficiencies that were up to 50 % higher than the common devices and showed no dependency on the particle type. As the particle concentrations for very small diameters between 2-4 nm

are below ~~5000~~10000 #/ccm, the charging efficiencies of the different devices vary strongly at these particle sizes. ~~However, the associated data points are in agreement with theory. This is not the case for NaCl particles as one can clearly see big variations~~ The nDMA in this size range has a low transmission efficiency ranging from 20-55 % and therefore the signal at the CPC 2 is very low. In addition, small temperature-fluctuations in the tube furnace lead to bigger uncertainties for the low total number concentration of the selected particle size. Especially for NaCl particles a big variation in the charging efficiencies of the different charging devices ~~. Those asymmetries~~ was observed. Those variations almost certainly are ~~owed to the low~~ caused by the low number concentrations of NaCl particles ~~with these sizes .~~ at these sizes compared to Ag particles. However, except for NaCl particles at particle diameters between 2-4 nm the associated data points for the ^{241}Am neutralizer agree well with the approximations by Tigges et al. (2015) and Wiedensohler (1988).

The charging efficiencies of the plasma torch for positively charged particles strongly differ from those of negatively charged particles. Again, the measured charging efficiencies of the soft X-Ray charger match almost perfectly with the theory for diameters between 4-12 nm. The ^{241}Am charger also agrees with the theoretically predicted values for diameters between 6-8 nm but shows asymmetries for larger particle sizes. The charging efficiency for positively charged particles decreases at larger sizes and results in lower values compared to theory for the ^{241}Am charger. The charging efficiencies of the plasma torch strongly depend on the type of working gas for positively charged particles. Evidently, the data using helium ~~agrees well~~ agree well with theoretical approximations from Tigges et al. (2015) and Wiedensohler (1988) in the size regime between 4 and 10 nm. For diameters between 10-12 nm the charging efficiencies even exceed the predicted values. The data suggest ~~that no dependency~~ no dependency of the charging efficiency on the charger ion polarity~~is present~~, when helium is used as working gas in the plasma torch. The data for compressed air match with the theoretical curves for the whole size range, and therefore behave similar to the soft X-Ray charger. As Figure 6 clearly shows, this will change drastically if nitrogen is used as the working gas. The charging efficiencies in positive polarity with nitrogen are significantly lower than with other chargers and other working gases in the whole size regime.

Wiedensohler and Fissan (1991) have shown that the predicted charging probabilities of NaCl and Ag particles strongly depend on the used carrier gas and the ion mass and mobility. During the ionization process positive ions and free electrons are formed from molecules in the carrier gas and ionized copper atoms. These primary ions attach to other molecules, as for example H_2O, CO_2, oxygen and halogens, and form bigger ion clusters that afterwards stick to the investigated particles. Wiedensohler and Fissan (1991) have shown that the variation of the ion masses leads to different theoretically predicted charging probabilities. For nitrogen as carrier gas they discovered a large dependency of the charging probability on the ion masses. Similar asymmetries are observed in our data when comparing the measured charging efficiencies of the plasma torch with nitrogen as working gas to the N_2 results of Wiedensohler and Fissan (1991). As Figure 3 shows, the plasma torch forms copper ions and free electrons which charge aerosol particles in the carrier gas. The significantly different masses of these ions may account for the differing charging efficiencies that are accomplished with nitrogen for the negatively as well as for the positively charged particles according to Wiedensohler (1988).

As the working gas flow is exposed to a high frequency electrical field before it mixes with the aerosol flow, the ions can form in a pure nitrogen environment~~almost~~ . Hence the charger ions form in a nitrogen atmosphere like in the ~~mentioned~~ case

Table 4. Comparison of ion cluster properties: polarity, mobility diameter D_p calculated from mean ion mobility Z, mean ion mass M and ion mobility ratio Z^-/Z^+.

	Polarity	D_p [nm]	Z [cm^2/Vs]	M [Da]	Z^-/Z^+	
Reischl et al. (1996)	+	1.32	1.15	290	1.0	0.80
Reischl et al. (1996)	-	1.19	1.43	140	1.0	0.80
measured	+	1.07	1.76	356	1.0	0.66
measured	-	0.87	2.66	116	1.0	0.66

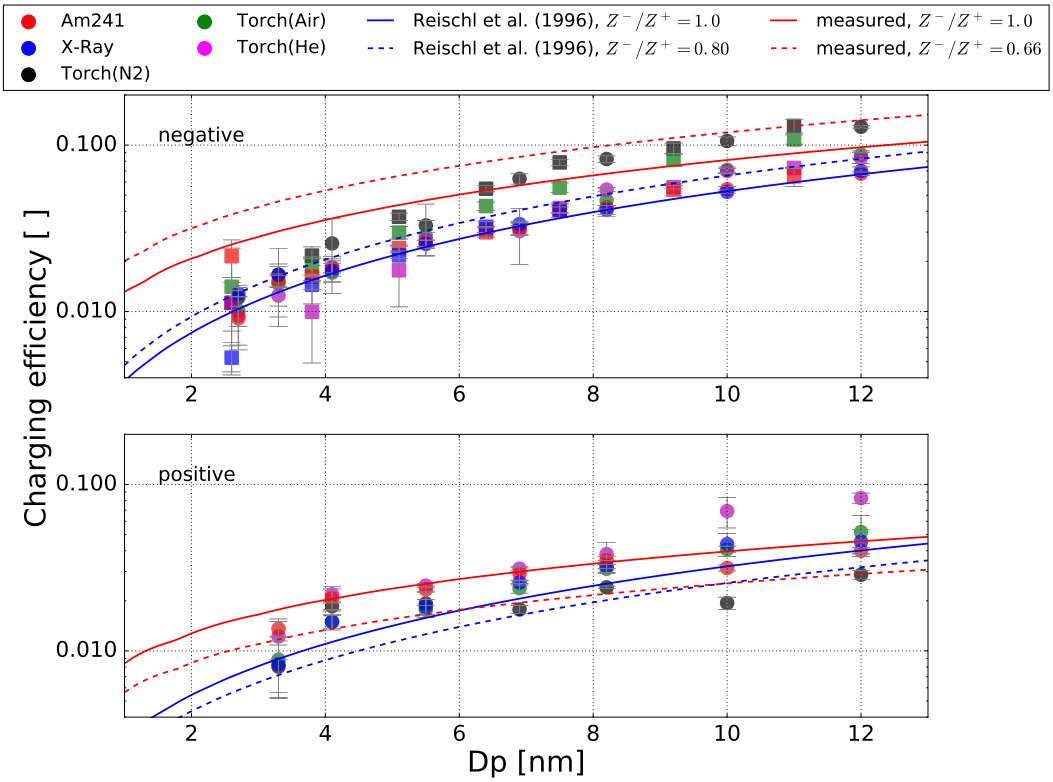

Figure 7. Measured charging efficiencies for the different aerosol chargers for negatively and positively charged Ag particles (dots) and negatively charged NaCl particles (squares) with mobility diameters less than 12 nm. The lines represent the charge distribution according to Fuchs theory, the parameters for the ion mobilities, ion masses and ion mobility ratio are listed in Table 4. The collision probability of ions was calculated following Hoppel and Frick (1986).

of Wiedensohler and Fissan (1991) where silver and sodium chloride particles were charged with a Kr 85 source in a pure nitrogen atmosphere. A similar but smaller effect was observed in atmospheric air as carrier gas. This mechanism would also explain the better charging efficiencies with ambient air as working gas.

In Table 4 the measured and calculated mean ion charger mobilities, mobility equivalent diameters, masses and ion mobility ratios are listed. For comparison the values found by Reischl et al. (1996) are also listed. The results were used to calculate the charge distribution with Fuchs theory as shown in Figure 7. Negatively charged particles in the size range from 4-12 nm by ^{241}Am or X-Ray neutralizers agree well with the parameters derived by Reischl et al. (1996) and an ion mobility ratio of 1. For positively charged particles the charging efficiency is below the measurement results for particles between 4-10 nm. By correcting the charge distribution with the parameters derived by Reischl et al. (1996) with an ion mobility ratio of 0.8 the negatively charged particles with a size below 4 nm fit perfectly to theory. The measurement results of this work reveal an increased charging efficiency for both polarities as shown in Figure 7. For mobility equivalent diameters between 4 and 12 nm and positive polarity the charging efficiency fits with theory for ^{241}Am, X-Ray and the plasma torch with air as working gas. In contrast to negatively charged particles where the results of the plasma torch with nitrogen or air as working gas above 7 nm is higher and below 7 nm is lower than expected by theory. Also, for ^{241}Am, X-Ray and the plasma charger with helium the theory exceeds the measured charging efficiency. By correcting the theory with the acquired ion mobility ratio, a good agreement between theory and measurement can be found for negatively charged particles above 7 nm and for positively charged particles for the plasma torch with nitrogen as working gas. Although the effect for diameters > 7 nm can be explained, there is still a deviation for the smaller diameters from theory. The reported discrepancy can therefore not solely be attributed to the ion mobilities. There are other effects which should by investigated in further studies. Especially the charging effects below 5 nm which cause deviations from the charging model.

Figure 8 depicts the recorded negatively charged aerosol size distribution averaged over numerous measurements, as well as the charging efficiency of the individual chargers normalized to the ^{241}Am charger recordings. The normalization was done by comparing the recorded total number concentration of the individual neutralizers with the recorded total number concentration of the ^{241}Am charger. The inversion of the size distribution data was ~~made~~ performed according to Petters (2018). These diagrams permit a qualitative descriptive comparison of the different charging devices. The left plot reveals a shift of about 1 nm in the maximum of the recorded size distribution between the X-Ray and the plasma charger~~.~~, which might be a result of small shifts in the size distribution originated from the tube furnace because of small temperature-fluctuations. Furthermore, contaminations of the X-Ray charger from previous experiments with ammonium sulfate might also lead to an increased particle diameter for the observed neutralizer (Steiner and Reischl, 2012). In addition, a significantly higher peak with the plasma torch was recorded which is most likely due to the higher charging efficiency at smaller sizes. Since the neutralizers were rotated periodically in multiple cycles, the possibility of systematic uncertainties in the actual size distribution was minimized. Therefore, the raised signal of the plasma torch can be attributed to a generally higher charging efficiency. The right plot simplifies a direct comparison of the plasma torch operated with different working gases and the soft X-Ray as well as the ^{241}Am charger as the calculated charging efficiencies are normalized to the ^{241}Am charger. The X-Ray charger is slightly less efficient than the radioactive ^{241}Am charger but still within the uncertainty range. This decrease can be attributed to the performance reduction during continuous operation which typically occurs during long measurement cycles. Compared to conventional chargers the plasma torch proves to charge slightly better with air as the working gas and less efficient with helium. With nitrogen as working gas, the plasma torch charges up to 50 % more than with air and helium and more than

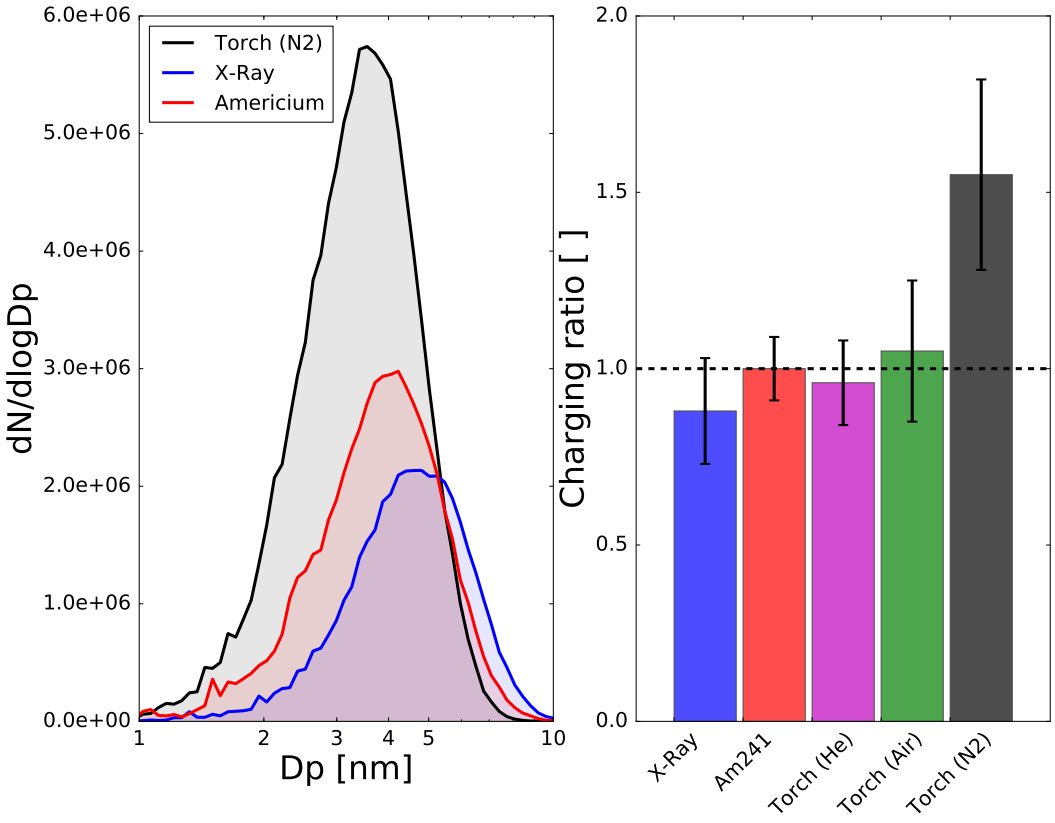

Figure 8. The plot on the left side represents the same recorded negative Ag aerosol size distribution with a UCPC, depending on the mobility diameter for the plasma torch (N2), X-Ray and americium neutralizers. On the right-hand side all conducted measurements with the same aerosol distribution are normalized to the ^{241}Am results for a direct comparison.

the other tested neutralizers. According to Maißer et al. (2015), nitric acid has an anomalously high gas phase acidity for its mass and can persist in the gas phase in higher concentrations than other low mass species. By using helium as working gas the concentration of nitrate ions in the gas phase is lower than in air or N_2 and therefore charge transport decreases. This is contrary to using N_2 as working gas where an increased charging efficiency up to 50% was measured.

Figure 9 shows the dependence of the charging efficiency for different aerosol flowrates and particle sizes. The charging efficiencies for particles in the sub-50 nm regime show a significant dependence on the aerosol flowrate. The different neutralizers have proven to be more sensitive to varying flow rates and a reduced residence time in the ionizing atmosphere (He and Dhaniyala, 2014; Kallinger et al., 2012; Kallinger and Szymanski, 2015).

Figure 9 reveals that the aerosol charging is most efficient for a flowrate of 2.5 L/Min and the charging efficiency decreases for higher flowrates. Kallinger and Szymanski (2015) and Jiang et al. (2014) also measured the flowrate dependence of different chargers. In the study by Kallinger and Szymanski (2015) an increased charging efficiency for the americium neutralizer for

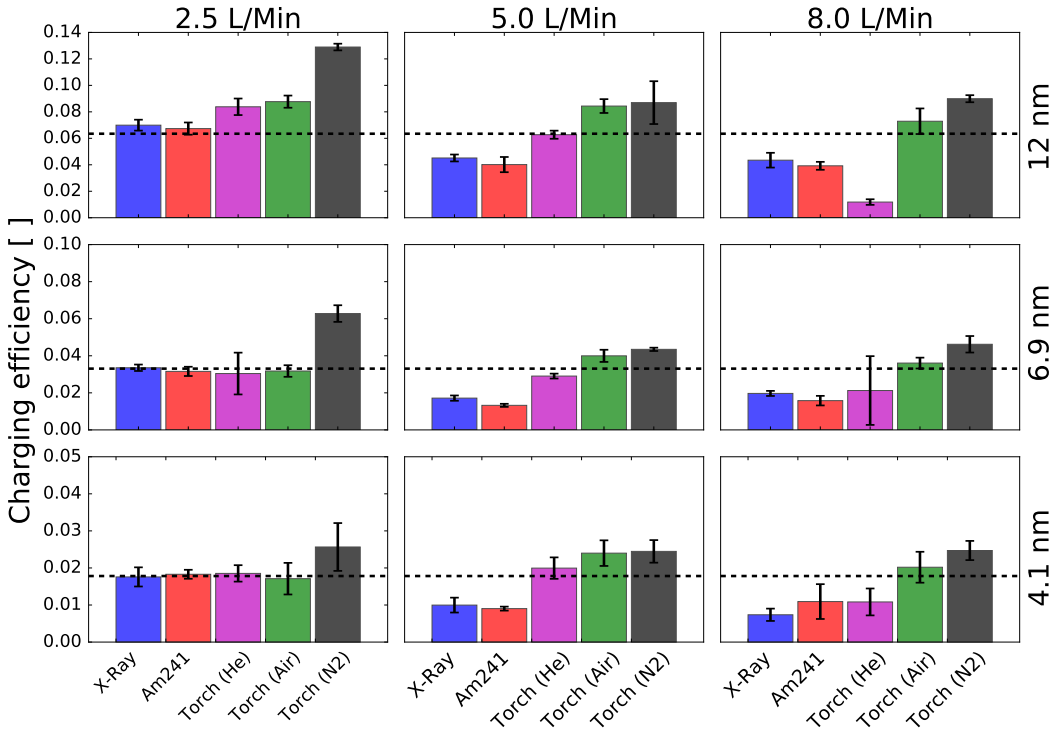

Figure 9. Measured charging efficiencies for the different aerosol chargers and aerosol flow rates for negatively charged Ag particles with mobility diameters of 12, 6.9 and 4.1 nm. The dotted black line represents the theoretical charging efficiency according to Wiedensohler (1988) for the 3 different mobility diameters.

a flowrate of 5.0 L/Min was found. In addition, contradictory to our findings, a reduced charging performance for the X-Ray neutralizer was not observed by Kallinger and Szymanski (2015) and Jiang et al. (2014). A reason for that could be a reduced charging due to low power output of the X-Ray tube. Since the last repair and calibration of the analyzed TSI 3088 neutralizer the operating run-time was about 371 hours. Furthermore, in this work, we used a different aerosol generation method compared to the above mentioned studies which could lead to different charging mechanism. Especially in the sub-10 nm size range different chemo-physical interactions might lead to unforseen results which should be investigated in future studies. The plasma torch also achieves the highest charging efficiencies for lower flowrates but seems to be not as sensitive to the aerosol flow compared to the other devices. Especially air and nitrogen have proven to be the most robust options as working gases.

3.3.1 ~~Charger ion chemical composition~~

~~Negative (left) and positive (right) mass spectra of ions generated by the ^{241}Am charger (first panel) and the plasma source for three different working gases, synthetic air (second panel), N_2 (third panel) and He (fourth panel) were measured using the setup in the upper panel of Figure 2. The mass spectra were averaged over 1 hour each. The identified compounds are labeled~~

in the second panel and are presented in Table 3. The negative mass spectrum was normalized to the NO_3^- ion (integer mass 62 Th), the positive mass spectrum was normalized to the $(H_2O)_2 \cdot H_3O^+$ cluster (integer mass 55 Th). The H_3O^+ ion is not displayed here since it was not covered by the set mass range of the ioniAPi-TOF. The dashed square box marks unidentified masses in the positive ^{241}Am mass spectrum and the solid square box shows the silicone compounds that are listed in Table 3.

The ion properties of ionic molecular clusters produced in the plasma torch were investigated by means of electrical mobility and mass spectrometry. Mobility spectra and mass spectra were recorded for positive and negative ions and compared to the resulting spectra from ions produced in the ^{241}Am charger. Figure 4 shows the mass spectra for negative (left) and positive (right) ions generated by the ^{241}Am charger (first panel) and the plasma torch for the three different working gases (second to fourth panel) using the setups shown in Figure 2 at the working gas flow settings presented in Table S1 and S2 in the supporting information (SI). The positive mass spectra were normalized to the nitrate ion (NO_3^-) peak at an integer mass of 62 Th and the negative mass spectra to the $(H_2O)_2 \cdot H_3O^+$ water cluster at an integer mass of 55 Th. The negative mass spectra are dominated by the nitrate ion, NO_3^-, and its dimer, trimer and water cluster (see labels in second panel in Figure 4). The three spectra for charger ions produced from the torch exhibit the same major peaks with the nitrate ion trimer peak being highest when He is used as working gas (see fourth panel). This observation may be a result of the different operational settings of the plasma torch when He is used as working gas (see Table S1 and S2). The negative ion spectrum of the Am241 charger reveals the same major peaks as the plasma torch negative mass spectra. Similar results have been found by a study investigating the chemical composition of ions produced by a corona discharge (Manninen et al., 2011). The identified major peaks of the positive mass spectra are listed in Table 3. In the lower mass range between 40 - 80 Th, protonated water, H_3O^+, and water clusters thereof dominate the spectrum for the ^{241}Am charger and the three spectra In addition to the flow dependent charging efficiency measurements, the ozone concentration was recorded with an O3-Monitor (Thermo Scientific Fischer, Model 49i). Elevated ozone concentration were observed at lower flow rates and for air as well as helium as working gas. In the case of air, a high amount of oxygen is present in the working gas of the plasma torch . The elemental composition of four major peaks in the positive spectra which supports the ozone production. For helium the afterglow of the plasma torch at integer masses of 88, 175, 187 and 201 Th were identified as carbonaceous compounds. In the higher mass range between 600 - 1000 Th, a set of major peaks was identified as silicone compounds. The same peaks were identified in the positive mass spectra of ions produced from the ^{241}Am charger (solid black box in Figure 4). This observation was also made by Manninen et al. (2011), who explain these peaks as a result of contamination from silicone tubing. Silicone tubing is oftentimes used in aerosol measurements and can cause artifacts because of degassing of siloxanes (Asbach et al., 2016). However, a range of peaks in the mass window from approximately 200 to 500 Th remains unidentified (dashed black box). These carbonaceous compounds have a positive mass defect and likely arise from ionization of constituents in the pressurized air that was used as carrier gas and the corresponding UV-light emission can be responsible for the increased amount of ozone. In addition, the applied electromagnetic field can cause a split of O_2 molecules. Especially, when the residence time is increased at low working gas flow rates. All recorded measurements can be found in the supporting material (Table S1).

The chemical composition of the plasma-generated ions was found to be independent of the choice of the working gas as shown in Figure 4. Also, the averaged electrical mobility measurements (averaged over 10 scans)conducted with the

experimental setup depicted in Figure 2 (lower panel) revealed identical peaks. The mobility spectra for the plasma torch using N_2, He and air as working gas and the ^{241}Am charger are presented in Figure 5. Similar results for different bipolar charging devices have been found by Kallinger et al. (2012) and Steiner and Reischl (2012). The latter have analysed the effects of carrier gas contaminants on the charging probability which influences the electrical mobility spectrum. One of the analysed TSI X-Ray charger showed a different mobility spectrum compared to the other analysed neutralizers. According to our mass spec analysis, this is due to ammonium sulfate contamination's from previous experiments which results in masses from $(NH_4)_2SO_4^-$ to $(NH_4)_{14}SO_4^-$.

Mobility distributions of the charger ions generated by the plasma torch using N_2, He and air as working gas and the ^{241}Am charger. The upper panel shows the mobility diameter distribution of the positive charger ions, the lower panel presents the mobility diameter distribution of the negative charger ions.

Overview of major negative and positive compounds in the mass spectra recorded using the ioniAPi-TOF in positive and negative ion mode. Integer m/z (Th) Molecular Formula Integer m/z (Th) Molecular Formula 46 NO_2^- 32 O_2+ 62 NO_3^- 37 $H_2O \cdot H_3O^+$ 80 $H_2O \cdot NO_3^-$ 55 $(H_2O)_2 \cdot H_3O^+$ 124 - 73 $(H_2O)_3 \cdot H_3O^+$ 125 $HNO_3 \cdot NO_3^-$ 88 $C_4H_{10}NO^+$ 187 - 175 $C_4H_9NO \cdot C_4H_{10}NO^+$ 188 $(HNO_3)_2 \cdot NO_3^-$ 187 $C_{10}H_{21}NO_2^+$ 201 $C_{11}H_{23}NO_2^+$ 610 $(SiOC_2H_6)_8OH_2^+$ 684 $(SiOC_2H_6)_9OH_2^+$ 758 $(SiOC_2H_6)_{10}OH_2^+$ 832 $(SiOC_2H_6)_{11}OH_2^+$ 906 $(SiOC_2H_6)_{12}OH_2^+$

4 Conclusions

The presented measurements conducted with a non-thermal plasma source ~~, americium and X-Ray neutralizer~~ have shown that ~~the different charging mechanisms~~ helium, nitrogen and air as working gases lead to the same ion species. According to the ~~API-MS measurements the same chemical compounds were formed with the different charger mechanisms.~~ mobility and mass spec measurements the comparison of the plasma charger with the americium neutralizer indicates the same negative ion species. Whereas for the positive ions the measurements reveal a slight deviation. At this point it should be noted that the chemical composition of the charger ions is affected by the tubing material and contaminations as discussed by Steiner and Reischl (2012).

It should be noted that the analyzed chemical composition of the neutralizer ions did not lead to changes in chemical composition even with increased ozone concentration caused by the plasma torch. By switching the working gas to nitrogen an increased charging efficiency could be recorded for negatively charged particles compared to ^{241}Am neutralizer. In accordance with Mathon et al. (2017), the ozone concentration can be reduced to ambient conditions with nitrogen which is beneficial for the commercial use. For future studies, the influence of the variation of the operational settings and the resulting ozone concentrations of the plasma torch remains to be investigated.

The higher charging probabilities for negatively charged particles in the size range from 7 to 12 nm can be attributed to differences in the electrical mobility. According to ~~Wiedensohler (1988)~~ our measurements the ratio of ion mobilities, given by the ion mobility of positively charged particles divided by the ion mobilities of negatively charged particles, yields a constant value of ~~0.875~~0.66. Consequently, the ion mobilities for negatively charged particles are on average higher. ~~The~~ This increased charging efficiency for negatively charged particles and decreased charging efficiency for positively charged particles was also measured by Wiedensohler and Fissan (1991) for Kr85 bipolar neutralizer in nitrogen. According to our measurements, similar results could be found for the plasma torch with nitrogen as working gas. The charging efficiency of the non-thermal atmospheric plasma source indicated a weak aerosol flow dependence when operated with nitrogen or compressed air in comparison to the americium and X-Ray neutralizers.

In summary, with different experimental approaches we were able to quantitatively characterize the Gilbert Mark I plasma source with nitrogen, helium and air as working gas. In addition, a commonly used X-Ray neutralizer and a radioactive americium neutralizer were analyzed for comparison. The highest charging efficiencies for negatively charged particles were found for the Gilbert Mark I plasma charger with nitrogen as working gas. Our results also reveal the importance of well characterized and clean neutralizers to avoid any misinterpretation of experimental data especially in the sub-10 nm size range. In addition, contrary to ozone suppression, the plasma source revealed great potential to act as an ozone generator by changing the working gas, for example, to argon.

Data availability. Supplementary data associated with this article can be found in the online version.

Author contributions. Christian Tauber designed the setup, Christian Tauber and David Schmoll performed the charging efficiency experiments, Johannes Gruenwald and David Schmoll performed the OES measurements, Christian Tauber and Sophia Brilke performed the mobility distribution measurements, Sophia Brilke and Daniela Wimmer performed the chemical composition measurements, Christian Tauber, David Schmoll, Johannes Gruenwald, Sophia Brilke, Peter Josef Wlasits, Daniela Wimmer and Paul Martin Winkler were involved in the scientific interpretation and discussion, and Christian Tauber, David Schmoll, Johannes Gruenwald, Sophia Brilke, Peter Josef Wlasits, Daniela Wimmer and Paul Martin Winkler wrote the manuscript.

Competing interests. The authors declare that they have no conflict of interest.

Acknowledgements. This work was supported by the Austrian Research Promotion Agency (FFG) under grant number 870121 and by the Austrian Science Fund (FWF) Project J3951-N36. The authors want to thank Peter Kallinger, Gruenwald Laboratories GmbH and Grimm Aerosol Technik Ainring GmbH & Co Kg for the support.

References

Adachi, M., Kousaka, Y., and Okuyama, K.: Unipolar and bipolar diffusion charging of ultrafine aerosol particles, Journal of Aerosol Science, 16, 109 – 123, https://doi.org/https://doi.org/10.1016/0021-8502(85)90079-5, http://www.sciencedirect.com/science/article/pii/0021850285900795, 1985.

Asbach, C., Kaminski, H., Lamboy, Y., Schneiderwind, U., Fierz, M., and Todea, A. M.: Silicone sampling tubes can cause drastic artifacts in measurements with aerosol instrumentation based on unipolar diffusion charging, Aerosol Science and Technology, 50, 1375–1384, 2016.

Barmpounis, K., Ranjithkumar, A., Schmidt-Ott, A., Attoui, M., and Biskos, G.: Enhancing the detection efficiency of condensation particle counters for sub-2nm particles, Journal of Aerosol Science, 117, 44 – 53, https://doi.org/https://doi.org/10.1016/j.jaerosci.2017.12.005, http://www.sciencedirect.com/science/article/pii/S0021850217300216, 2018.

Brilke, S., Resch, J., Leiminger, M., Steiner, G., Tauber, C., Wlasits, P. J., and Winkler, P. M.: Precision characterization of three ultrafine condensation particle counters using singly charged salt clusters in the 1–4 nm size range generated by a bipolar electrospray source, Aerosol Science and Technology, 54, 396–409, https://doi.org/10.1080/02786826.2019.1708260, https://doi.org/10.1080/02786826.2019.1708260, 2020.

Cooper, D. W. and Reist, P. C.: Neutralizing charged aerosols with radioactive sources, Journal of Colloid and Interface Science, 45, 17 – 26, https://doi.org/https://doi.org/10.1016/0021-9797(73)90239-7, http://www.sciencedirect.com/science/article/pii/0021979773902397, 1973.

Deka, T., Boruah, A., Sharma, S. K., and Bailung, H.: Observation of self-excited dust acoustic wave in dusty plasma with nanometer size dust grains, Physics of Plasmas, 24, 093 706, https://doi.org/10.1063/1.5001721, https://aip.scitation.org/doi/10.1063/1.5001721, 2017.

Fernández de la Mora, J. and Barrios-Collado, C.: A bipolar electrospray source of singly charged salt clusters of precisely controlled composition, Aerosol Science and Technology, 51, 778–786, https://doi.org/10.1080/02786826.2017.1302070, 2017.

Flagan, R. C.: On Differential Mobility Analyzer Resolution, Aerosol Science and Technology, 30, 556–570, https://doi.org/10.1080/027868299304417, https://doi.org/10.1080/027868299304417, 1999.

Fuchs, N. A., Daisley, R. E., Fuchs, M., Davies, C. N., and Straumanis, M. E.: The Mechanics of Aerosols, Physics Today, 18, 73, https://doi.org/10.1063/1.3047354, https://doi.org/10.1063/1.3047354, 1965.

Gruenwald, J., Reynvaan, J., Eisenberg, T., and Geistlinger, P.: Characterisation of a Simple Non-Thermal Atmospheric Pressure Plasma Source for Biomedical Research Applications, Contributions to Plasma Physics, 55, 337–346, https://doi.org/10.1002/ctpp.201400059, https://onlinelibrary.wiley.com/doi/abs/10.1002/ctpp.201400059, 2015.

Harper, J. D., Charipar, N. A., Mulligan, C. C., Zhang, X., Cooks, R. G., and Ouyang, Z.: Low-Temperature Plasma Probe for Ambient Desorption Ionization, Analytical Chemistry, 80, 9097–9104, https://doi.org/10.1021/ac801641a, https://doi.org/10.1021/ac801641a, pMID: 19551980, 2008.

He, M. and Dhaniyala, S.: Experimental characterization of flowrate-dependent bipolar diffusion charging efficiencies of sub-50nm particles, Journal of Aerosol Science, 76, 175 – 187, https://doi.org/https://doi.org/10.1016/j.jaerosci.2014.06.009, http://www.sciencedirect.com/science/article/pii/S0021850214001062, 2014.

Hoppel, W. A. and Frick, G. M.: Ion—Aerosol Attachment Coefficients and the Steady-State Charge Distribution on Aerosols in a Bipolar Ion Environment, Aerosol Science and Technology, 5, 1–21, https://doi.org/10.1080/02786828608959073, https://doi.org/10.1080/02786828608959073, 1986.

Intra, P. and Yawootti, A.: An Experimental Investigation of A Non-Mixing Type Corona-Needle Charger for Submicron Aerosol Particles, Journal of Electrical Engineering and Technology, 14, 1–8, https://doi.org/10.1007/s42835-018-00011-x, 2019.

Jiang, J., Kim, C., Wang, X., Stolzenburg, M. R., Kaufman, S. L., Qi, C., Sem, G. J., Sakurai, H., Hama, N., and McMurry, P. H.: Aerosol Charge Fractions Downstream of Six Bipolar Chargers: Effects of Ion Source, Source Activity, and Flowrate, Aerosol Science and Technology, 48, 1207–1216, https://doi.org/10.1080/02786826.2014.976333, https://doi.org/10.1080/02786826.2014.976333, 2014.

Junninen, H., Ehn, M., Petäjä, Luosujärvi, L., Kotiaho, T., Kostiainen, R., Rohner, U., Gonin, M., Fuhrer, K., Kulmala, M., and Worsnop, D. R.: A high-resolution mass spectrometer to measure atmospheric ion composition, Atmospheric Measurement Techniques, 3, 1039–1053, https://doi.org/10.5194/amt-3-1039-2010, 2010.

Kallinger, P. and Szymanski, W.: Experimental determination of the steady-state charging probabilities and particle size conservation in non-radioactive and radioactive bipolar aerosol chargers in the size range of 5–40 nm, Journal of Nanoparticle Research, 17, https://doi.org/10.1007/s11051-015-2981-x, 2015.

Kallinger, P., Steiner, G., and Szymanski, W.: Characterization of four different bipolar charging devices for nanoparticle charge conditioning, Journal of Nanoparticle Research, 14, https://doi.org/10.1007/s11051-012-0944-z, 2012.

Kopnin, S. I., Morozova, T. I., and Popel, S. I.: Electron Beam Action and High Charging of Dust Particles, IEEE Transactions on Plasma Science, 46, 701–703, https://doi.org/10.1109/TPS.2017.2748378, 2018.

Kramida, A., Ralchenko, Y., Reader, J., and NIST, N. A. T.: Atomic spectra and ionization energies of the elements, https://physics.nist.gov/PhysRefData/ASD/, 2013.

Kurake, N., Tanaka, H., Ishikawa, K., Kondo, T., Sekine, M., Nakamura, K., Kajiyama, H., Kikkawa, F., Mizuno, M., and Hori, M.: Cell survival of glioblastoma grown in medium containing hydrogen peroxide and/or nitrite, or in plasma-activated medium, Archives of Biochemistry and Biophysics, 605, 102 – 108, https://doi.org/https://doi.org/10.1016/j.abb.2016.01.011, http://www.sciencedirect.com/science/article/pii/S000398611630011X, special Issue: Low-temperature plasma in biology and medicine, 2016.

Leiminger, M., Feil, S., Mutschlechner, P., Ylisirniö, A., Gunsch, D., Fischer, L., Jordan, A., Schobesberger, S., Hansel, A., and Steiner, G.: Characterisation of the transfer of cluster ions through an atmospheric pressure interface time-of-flight mass spectrometer with hexapole ion guides, Atmospheric Measurement Techniques, 12, 5231–5246, https://doi.org/10.5194/amt-12-5231-2019, https://www.atmos-meas-tech.net/12/5231/2019/, 2019.

Liu, B. Y. and Pui, D. Y.: Electrical neutralization of aerosols, Journal of Aerosol Science, 5, 465 – 472, https://doi.org/https://doi.org/10.1016/0021-8502(74)90086-X, http://www.sciencedirect.com/science/article/pii/002185027490086X, 1974.

Maißer, A., Thomas, J. M., Larriba-Andaluz, C., He, S., and Hogan, C. J.: The mass–mobility distributions of ions produced by a Po-210 source in air, Journal of Aerosol Science, 90, 36 – 50, https://doi.org/https://doi.org/10.1016/j.jaerosci.2015.08.004, http://www.sciencedirect.com/science/article/pii/S0021850215001305, 2015.

Manninen, H. E., Franchin, A., Schobesberger, S., Hirsikko, A., Hakala, J., Skromulis, A., Kangasluoma, J., Ehn, M., Junninen, H., Mirme, A., Mirme, S., Sipilä, M., Petäjä, T., Worsnop, D. R., and Kulmala, M.: Characterisation of corona-generated ions used in a Neutral cluster and Air Ion Spectrometer (NAIS), Atmospheric Measurement Techniques, 4, 2767–2776, https://doi.org/10.5194/amt-4-2767-2011, https://www.atmos-meas-tech.net/4/2767/2011/, 2011.

Mathon, R., Jidenko, N., and Borra, J.-P.: Ozone-free post-DBD aerosol bipolar diffusion charger: Evaluation as neutralizer for SMPS size distribution measurements, Aerosol Science and Technology, 51, 282–291, https://doi.org/10.1080/02786826.2016.1265082, https://www.tandfonline.com/doi/full/10.1080/02786826.2016.1265082, 2017.

Michau, A., Arnas, C., Lombardi, G., Bonnin, X., and Hassouni, K.: Nanoparticle formation and dusty plasma effects in DC sputtering discharge with graphite cathode, Plasma Sources Science and Technology, 25, 015 019, https://doi.org/10.1088/0963-0252/25/1/015019, https://doi.org/10.1088%2F0963-0252%2F25%2F1%2F015019, 2016.

Petters, M. D.: A language to simplify computation of differential mobility analyzer response functions, Aerosol Science and Technology, 52, 1437–1451, https://doi.org/10.1080/02786826.2018.1530724, https://doi.org/10.1080/02786826.2018.1530724, 2018.

Reischl, G., Mäkelä, J., Karch, R., and Necid, J.: Bipolar charging of ultrafine particles in the size range below 10 nm, Journal of Aerosol Science, 27, 931 – 949, https://doi.org/https://doi.org/10.1016/0021-8502(96)00026-2, http://www.sciencedirect.com/science/article/pii/0021850296000262, fuchs Memorial Issue, 1996.

Spencer, S. E., Tyler, C. A., Tolocka, M. P., and Glish, G. L.: Low-Temperature Plasma Ionization-Mass Spectrometry for the Analysis of Compounds in Organic Aerosol Particles, Analytical Chemistry, 87, 2249–2254, https://doi.org/10.1021/ac5038889, https://doi.org/10.1021/ac5038889, pMID: 25587636, 2015.

Steiner, G. and Reischl, G. P.: The effect of carrier gas contaminants on the charging probability of aerosols under bipolar charging conditions, Journal of Aerosol Science, 54, 21 – 31, https://doi.org/https://doi.org/10.1016/j.jaerosci.2012.07.008, http://www.sciencedirect.com/science/article/pii/S0021850212001334, 2012.

Steiner, G., Attoui, M., Wimmer, D., and Reischl, G. P.: A Medium Flow, High-Resolution Vienna DMA Running in Recirculating Mode, Aerosol Science and Technology, 44, 308–315, https://doi.org/10.1080/02786821003636763, https://doi.org/10.1080/02786821003636763, 2010.

Tauber, C., Brilke, S., Wlasits, P., Bauer, P., Köberl, G., Steiner, G., and Winkler, P.: Humidity effects on the detection of soluble and insoluble nanoparticles in butanol operated condensation particle counters, Atmospheric Measurement Techniques, 12, 3659–3671, https://doi.org/10.5194/amt-12-3659-2019, 2019a.

Tauber, C., Steiner, G., and Winkler, P. M.: Counting efficiency determination from quantitative intercomparison between expansion and laminar flow type condensation particle counter, Aerosol Science and Technology, 53, 344–354, https://doi.org/10.1080/02786826.2019.1568382, https://www.tandfonline.com/doi/full/10.1080/02786826.2019.1568382, 2019b.

Thomas, J. M., Chen, X., Maißer, A., and Hogan, C. J.: Differential heat and mass transfer rate influences on the activation efficiency of laminar flow condensation particle counters, International Journal of Heat and Mass Transfer, 127, 740 – 750, https://doi.org/https://doi.org/10.1016/j.ijheatmasstransfer.2018.07.002, http://www.sciencedirect.com/science/article/pii/S0017931018317101, 2018.

Tigges, L., Wiedensohler, A., Weinhold, K., Gandhi, J., and Schmid, H.-J.: Bipolar charge distribution of a soft X-ray diffusion charger, Journal of Aerosol Science, 90, 77 – 86, https://doi.org/https://doi.org/10.1016/j.jaerosci.2015.07.002, http://www.sciencedirect.com/science/article/pii/S0021850215001081, 2015.

Uner, N. B. and Thimsen, E.: In-Flight Size Focusing of Aerosols by a Low Temperature Plasma, The Journal of Physical Chemistry C, 121, 12 936–12 944, https://doi.org/10.1021/acs.jpcc.7b03572, https://pubs.acs.org/doi/abs/10.1021/acs.jpcc.7b03572, 2017.

Wang, S. C. and Flagan, R. C.: Scanning Electrical Mobility Spectrometer, Aerosol Science and Technology, 13, 230–240, https://doi.org/10.1080/02786829008959441, https://doi.org/10.1080/02786829008959441, 1990.

Wiedensohler, A.: An approximation of the bipolar charge distribution for particles in the submicron size range, Journal of Aerosol Science, 19, 387 – 389, https://doi.org/https://doi.org/10.1016/0021-8502(88)90278-9, http://www.sciencedirect.com/science/article/pii/0021850288902789, 1988.

Wiedensohler, A. and Fissan, H. J.: Bipolar Charge Distributions of Aerosol Particles in High-Purity Argon and Nitrogen, Aerosol Science and Technology, 14, 358–364, https://doi.org/10.1080/02786829108959498, https://doi.org/10.1080/02786829108959498, 1991.

Wiedensohler, A., Lütkemeier, E., Feldpausch, M., and Helsper, C.: Investigation of the bipolar charge distribution at various gas conditions, Journal of Aerosol Science, 17, 413 – 416, https://doi.org/https://doi.org/10.1016/0021-8502(86)90118-7, http://www.sciencedirect.com/science/article/pii/0021850286901187, 1986.

Winkler, P. M., Steiner, G., Vrtala, A., Vehkamäki, H., Noppel, M., Lehtinen, K. E. J., Reischl, G. P., Wagner, P. E., and Kulmala, M.: Heterogeneous Nucleation Experiments Bridging the Scale from Molecular Ion Clusters to Nanoparticles, Science, 319, 1374–1377, https://doi.org/10.1126/science.1149034, http://science.sciencemag.org/content/319/5868/1374, 2008.

Winklmayr, W., Reischl, G. P., Lindner, A., and Berner, A.: A new electromobility spectrometer for the measurement of aerosol size distributions in the size range from 1 to 1000 nm, Journal of Aerosol Science, 22, 289–296, https://doi.org/10.1016/S0021-8502(05)80007-2, 1991.

Yang, W., Zhu, R., and Ma, B.: Repetitively Pulsed Discharges Ignited in Microchannels Between Two Nonequally Broad Planar Electrodes and Their Charging for Nanoscale Aerosol Particles, IEEE Transactions on Plasma Science, 44, 944–949, https://doi.org/10.1109/TPS.2016.2560223, 2016.

Yaroshenko, V., Meier, P., Lühr, H., and Motschmann, U.: Physical Processes in the Dusty Plasma of the Enceladus Plume, pp. 241–262, Springer International Publishing, Cham, https://doi.org/10.1007/978-3-319-64292-5_9, https://link.springer.com/chapter/10.1007/978-3-319-64292-5_9, 2018.